



## Stabilization of reactive species by supramolecular encapsulation

Journal:	<i>Chemical Society Reviews</i>
Manuscript ID	CS-REV-11-2015-000861.R1
Article Type:	Review Article
Date Submitted by the Author:	12-Jan-2016
Complete List of Authors:	Galán, Albano; Institute of Chemical Research of Catalonia (ICIQ), The Barcelona Institute of Science and Technology Ballester, Pablo; Institute of Chemical Research of Catalonia (ICIQ), The Barcelona Institute of Science and Technology; Catalan Institution for Research and Advanced Studies (ICREA)



Journal Name

ARTICLE

## Stabilization of reactive species by supramolecular encapsulation

Albano Galan<sup>a</sup> and Pablo Ballester<sup>\*a,b</sup>Received 00th January 20xx,  
Accepted 00th January 20xx

DOI: 10.1039/x0xx00000x

www.rsc.org/

Molecular containers have attracted the interest of supramolecular chemists since the early beginnings of the field. Cavitands' inner cavities were quickly exploited by Cram and Warmuth to construct covalent containers able to stabilize and assist the characterization of short-lived reactive species such as cyclobutadiene or *o*-benzynes. Since then, more complex molecular architectures have been prepared able to store and isolate a myriad of fleeting species (i.e. organometallic compounds, cationic species, radical initiators...). In this review we cover selected examples of the stabilization of reactive species by encapsulation in molecular containers from the first reports of covalent containers described by Cram et al. to the most recent examples of containers with self-assembled structure (metal coordination cages and hydrogen bonded capsules). Finally, we briefly review examples reported by Rebek et al. in which elusive reaction intermediates could be detected in the inner cavities of self-folding resorcin[4]arene cavitands by the formation of covalent host-guest complexes. The utilization of encapsulated reactive species in catalysis or synthesis is not covered.

### Introduction

The inner cavity of a molecular container offers an isolated microenvironment wherein encapsulated guests are exposed to a reduced number of interactions compared to the bulk solution.<sup>1</sup> Whereas bound guests may interact only with the host or other co-encapsulated guests, in the bulk guests display a high number of interactions with solvent molecules or other guests. As a consequence, the properties of the bound guests are usually altered leading to applications for the resulting encapsulation complexes in different areas of chemical research that include: reactivity modulation<sup>1,2,3</sup> drug delivery,<sup>4</sup> mechanistic studies of chemical reactions,<sup>5,6,7</sup> reaction catalysis,<sup>8,9,10</sup> and selective organic synthesis.<sup>11,12,13</sup> Among them, the stabilization of reactive species represents an extremely relevant feature that is almost exclusive to molecular containers. Rebek distinguished between two different mechanisms in the stabilization of reactive species or transient reaction intermediates by encapsulation in a molecular container: a) stabilization of kinetically stable but reactive species that are not able to interact with solvent molecules, water, themselves... because of the constrictive

binding of the container (*shield* type) and b) stabilization of kinetically labile species in which the energy of the host-guest complex is lowered (*enzyme* type).<sup>14</sup> However, in many cases the separation of kinetic and thermodynamic phenomena controlling the stabilization may be difficult.<sup>15</sup>

During the last decades, the preparation of molecular containers have evolved from the initial fully covalent designs to more complex and elegant self-assembled architectures that rely on non-covalent interactions such as hydrogen bonding or metal-ligand coordination.

In this review we will focus on examples of the stabilization of reactive species by discrete and soluble supramolecular containers possessing a well-defined inner cavity that completely surrounds the encapsulated guest. The stabilization of short-lived species by metal-organic frameworks,<sup>16,17</sup> porous networks,<sup>18,19,20</sup> dendrimers,<sup>21</sup> cucurbiturils,<sup>22,23</sup> cyclodextrins<sup>24,25</sup> or solid-state capsules<sup>26</sup> fall out of the scope of this review. For the sake of brevity, examples related to the stabilization of high-energy conformers,<sup>27,28,29,30,31</sup> geometrical isomers,<sup>32</sup> tautomers,<sup>33,34,35</sup> unusual metal oxidation/spin states,<sup>36,37,38</sup> or non-covalently bonded aggregates<sup>39,40</sup> will not be discussed. Likewise, the use of reversible molecular encapsulation as a tool for the selective functionalization<sup>11,12,13,41,42,43,44,45,46</sup> of stable chemical entities and in the catalysis of chemical reactions<sup>8,9,10</sup> will not be reviewed.

The review is divided in three sections, corresponding to the different nature of the reviewed molecular containers. Firstly, we will discuss the stabilization of reactive species by encapsulation in covalent organic containers. We will cover from the early examples reported by Cram and Warmuth to more recent ones describing receptors with inner-cavity

<sup>a</sup> Institute of Chemical Research of Catalonia (ICIQ), The Barcelona Institute of Science and Technology  
Avgda. Països Catalans 16, 43007 Tarragona, Spain  
E-mail: pballester@iciq.es

<sup>b</sup> Catalan Institution for Research and Advanced Studies (ICREA)  
Passeig Lluís Companys 23, 08010 Barcelona, Spain

functionalization. Secondly, we will discuss the stabilization of reactive species by encapsulation in self-assembled molecular containers. The use of coordination cages and hydrogen bonded capsules will be covered. Finally, we will briefly comment on the stabilization of elusive reaction intermediates inside the cavities of unimolecular resorcin[4]arene cavitands through the formation of covalent host-guest complexes. The nature of the stabilized encapsulated guests covers reactive organometallic, inorganic and organic compounds, either ionic or neutral. The selected examples represent a broad overview of the utilization in solution of structurally well-defined containers for the stabilization of reactive species. The reactive species can be generated “in the cavity” from previously encapsulated non-reacting precursors, directly sequestered from the bulk solution by the container or emerge from the reaction of the container with the encapsulated cargo. We avoided the description of encapsulated species that have been used in reaction catalysis and synthetic applications.

## Stabilization of reactive species within covalent containers

### Containers based on resorcin[4]arene scaffolds: carcerands

The synthesis of the first molecular containers dates back to the early 90s. The connection of two resorcin[4]arene cavitands with covalent linkers afforded molecular containers with spherical and hollow cavities ideal for the entrapment of small guests.<sup>47</sup> Cram coined the term *carcerands* (from the Latin *carcer*, prison) to describe this new family of compounds because of the high kinetic stability of their host-guest complexes.<sup>48</sup> Preparation of carcerand-guest complexes (carceplexes) was achieved by either heating a mixture of the empty carcerand and the guest or by performing the shell-closing reaction affording the carcerand in the presence of the guest acting as a template. The efficient synthesis of carceplexes was controlled by the guest size (minimum steric interactions and complementarity between guest and host) and the number of van der Waals interactions established on complex formation.<sup>49</sup> It became clear very quickly that the properties of the trapped guests were very different from those in the bulk solution. Cram even talked about a *new phase of matter* to describe carcerands' inner cavities.<sup>50</sup> The stabilization of cyclobutadiene in the inner space of a carcerand was the first milestone in the stabilization of reactive species by molecular encapsulation and it was considered a major breakthrough in the newly born research field of molecular encapsulation.<sup>51</sup> Cyclobutadiene (**2**, Figure 1) is a very reactive diene that undergoes rapid thermal cyclization and ring expansion to afford cyclooctatetraene (**4**).

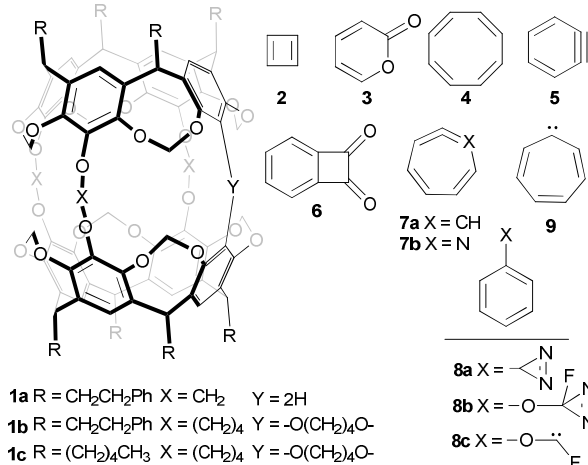
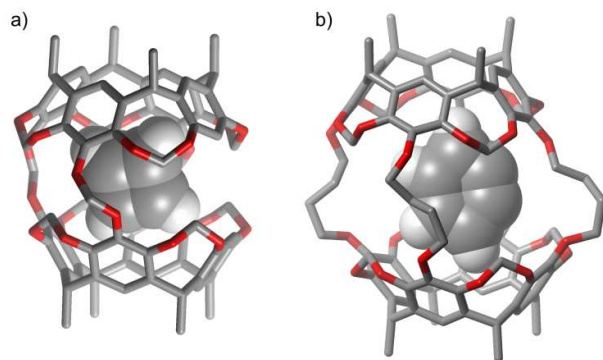


Figure 1. Line-drawing structures of the carcerands and guests used by Cram and Warmuth.

Before its stabilization in a molecular container, its existence had been proved only in an argon matrix at 8K.<sup>52</sup> In an elegant approach, Cram encapsulated  $\alpha$ -pyrone **3** within the aromatic walls of carcerand **1a** by refluxing empty **1a** in a CDCl<sub>3</sub> solution of **3**. After irradiation of the carceplex **3**⊂**1a** in a sealed NMR tube with a xenon lamp for 30 minutes, cyclobutadiene was produced within the container by extrusion of a molecule of CO<sub>2</sub> (Figure 2a). The formation of **2** in the inner cavity allowed the first spectroscopic characterization of cyclobutadiene. The observation of one singlet in the <sup>1</sup>H NMR spectrum ( $\delta$  = 2.27 ppm) for bound **2** and sharp signals for the host indicated that the guest was rotating rapidly on the NMR time scale within the cavity and in the singlet ground state. Bound cyclobutadiene was thermally stable at room temperature and up to 60 °C. However, when a THF solution of the **2**⊂**1a** carceplex was heated at 220 °C in a sealed NMR tube, bound cyclobutadiene was exchanged by a molecule of solvent from the bulk and the formation of cyclooctatetraene (**4**) was observed. The stabilization of cyclobutadiene arose from the constrictive binding of the capsule: at room temperature the bound guest could not escape through the narrow portals of the carcerand shell. However, at elevated temperatures, the bond's vibrations increased providing wider openings of the shell portals. This allowed the solvent's exchange and release of the bound cyclobutadiene to the bulk affording cyclooctatetraene **4**. It is interesting to note that in the presence of oxygen, cyclobutadiene was quickly oxidized even when bound in the cavity of **1a**. Oxygen is small enough to squeeze through the portals of the cavitand resulting in the oxidation of bound cyclobutadiene.

Inspired by the seminal work of Cram, Warmuth sought the stabilization of other fleeting species in the inner spaces of carcerands and hemicarcerands. Whereas at that time much effort was directed towards the isolation and characterization of intriguing *o*-benzyne (**5**, Figure 1) its detection was only possible at cryogenic temperatures (< -150 °C) and by a reduced number of spectroscopic techniques (IR, UV/Vis, solid-state <sup>13</sup>C NMR). Warmuth observed that benzyne's precursor **6**

was encapsulated within container **1b** in a moderate yield (ca. 30%). Upon light irradiation of a solution of the complex **6c1b**, *o*-benzyne **5** was generated within the carcerand cavity (Figure 2b). In the carceplex **5c1b** the encapsulated benzyne was stabilized and it was characterized spectroscopically in solution at -75 °C (<sup>1</sup>H and <sup>13</sup>C NMR). The encapsulated benzyne had a half-life of 205 s (calculated from the rate constant of the decay of its proton signal). However, at room temperature, bound **5** reacted rapidly with the interior of the host through an intramolecular Diels-Alder reaction.<sup>53</sup> The electronic nature of *o*-benzyne (acetylenic vs. cumulenic) was not clear with the data available at that time. Warmuth's findings in combination with theoretical calculations indicated that **5** had mainly an acetylenic structure.<sup>54,55</sup>



**Figure 2.** Energy-minimized (MM3) structures of the hemicarceplex a) **2c1a** and the carceplex b) **5c1b**. Substituents at the lower rim were truncated to methyl groups for simplicity. Hydrogen atoms of the host are removed for clarity. The host is depicted in stick representation and guest as CPK model.

In a similar manner, Warmuth reported the stabilization of the reactive 1,2,4,6-cycloheptatetraene (**7a**, Figure 1) by encapsulation in carcerand **1c**.<sup>56</sup> Whereas **7a** dimerized rapidly at temperatures higher than 15 K, when generated within the cavity of **1c**, the reactive allene was stable for weeks at room temperature and even for a reduced time at 100 °C.<sup>57</sup> Generation of the **7a****c1c** encapsulation complex occurred after light irradiation of the precursor carceplex **8a****c1c**. Interestingly, bound **7a** was stable at 60 °C 3 hours after the addition of methanol. Contrary to the experimental findings, a rapid reaction between bound **7a** and methanol was expected. The reduced size of methanol may allow its passage through the opening portals of **1c**. The authors proposed that whereas in solution species **7a** was involved in a fast equilibrium with **9**, in the inner cavity of **1c** the equilibrium was displaced towards **7a**. Theoretical calculations demonstrated that the polar cycloheptatrienyl carbene **9** was more reactive towards alcohols than the non-polar tetraene **7a**.<sup>57</sup> Experiments using chiral carcerands set a lower limit of 19.6 kcal mol<sup>-1</sup> for the energy difference between the hemicarceplexes of tetraene **7a** and carbene **9**.<sup>57</sup> The absence of species **9** within the carcerand explained the stabilization towards methanol. Nevertheless, even if the allenic species **7a** was not reactive towards methanol, it was air-sensitive. In agreement, when a solution of carceplex **7a****c1c** was exposed to air, bound **7a** was rapidly

oxidized to yield the benzene hemicarceplex and CO<sub>2</sub>. The oxygen molecule is small enough to enter the inner cavity of **1c** through its portals.

In a similar example, irradiation of carceplex **8b****c1c** produced the *in situ* formation of the incarcerated complex **8c****c1c**. The transient fluorophenoxycarbene (**8c**) was stabilized in the inner cavity and persisted for days at room temperature.<sup>58</sup> Also, Warmuth described the stabilization of the reactive 1-azacyclohepta-1,2,4,6-tetraene **7b** in the inner cavity of carcerand **1c** but no kinetic or thermodynamic data were provided about its stabilization.<sup>59,60</sup> Other reactive molecules that were stabilized in the inner phase of carcerands were anti-Bredt's olefins i.e. bicyclo[2.2.2]oct-1-ene (**10**, Figure 3).<sup>61</sup>

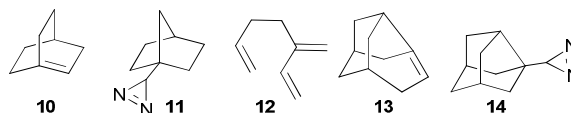


**Figure 3.** Line-drawing structures of anti-Bredt's olefins and related molecules described in Warmuth's works.

Anti-Bredt's olefins contain a double bond in a bridgehead position, which makes them highly strained and very unstable. Anti-Bredt olefin **10** rapidly dimerizes or undergoes a retro Diels-Alder reaction to afford **12**, which complicated its detection. Warmuth prepared a solution of carceplex **11c1b**, containing carbene precursor **11**. After irradiation of a solution of **11c1b**, a new carceplex containing the reactive species **10** was detected (ca. 20% yield). Even if bound **10** was rapidly oxidized, the increase in its thermal stability was remarkable. Warmuth et al. calculated the rate constant for the retro Diels-Alder (**10** to **12**) of bound **10** at 61.7 °C to be  $k = 2.2 \times 10^{-5} \text{ s}^{-1}$ . This represented a large increase of more than 2000-fold in the thermal stability of bound **10** when compared to the free species. The authors attributed the high kinetic stability of bound **10** to the tight and narrow environment provided by the cavity that energetically disfavored the transition state required for the retro Diels-Alder reaction.

In a more complex design, Warmuth pursued the stabilization of the short-lived olefin protoadamantane (**13**, Figure 3), which rapidly dimerizes in solution. The carbene precursor **14** was readily encapsulated in the dynamic covalent self-assembled container **15** (Figure 4a). Capsule **15** is covalently linked through imine bonds and bears eight sulphate groups at the lower rims of the resorcin[4]arene scaffolds, which rendered the receptor water-soluble.

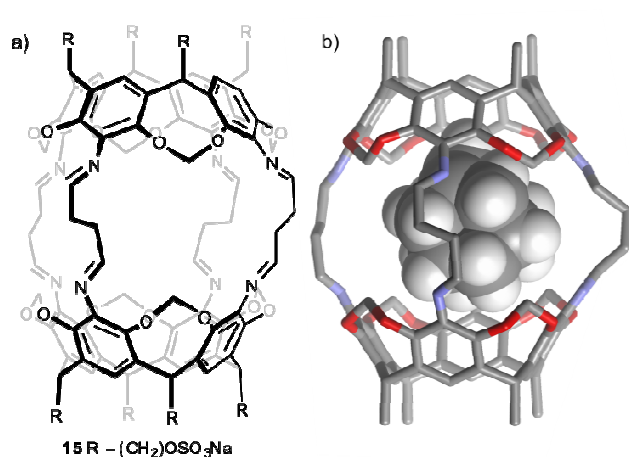


**Figure 4.** a) Line-drawing structure of water-soluble dynamic covalent container **15** prepared by Warmuth et al. b) Energy-minimized (MM3) structure of the complex **13@15**. Substituents at the lower rim were truncated to methyl groups for simplicity. Hydrogen atoms of the host are removed for clarity. The host is depicted in stick representation and guest shown as CPK model.

Interestingly, the encapsulation complex **14@15** was observed even in D<sub>2</sub>O, evidencing that the template effect was strong enough to overcome the unfavorable imine formation in water. When a 1:1 DMSO-*d*<sub>6</sub>/CD<sub>3</sub>CN solution of the complex **14@15** was irradiated ( $\lambda = 350$  nm), a new encapsulated species emerged in the <sup>1</sup>H NMR spectrum of the solution. 2D NMR spectroscopy allowed the assignment of the new signals to the protons of the complex **13@15** (Figure 4b). This result indicated that the elusive protoadamantane **13** was generated and stabilized within the container and could be spectroscopically detected. The half-life of bound **13** was 5.5 days at room temperature. More impressive, the assembly **13@15** was even formed in D<sub>2</sub>O ( $t_{1/2} = 5$  min, 5 °C). The rate of decomposition of the encapsulation complex was similar to the rate of imine hydrolysis, which indicated that the stabilization of the guest was controlled by the stability of the imine bonds that held together the components of the molecular capsule. These results highlighted once more that the stabilization of reactive species by encapsulation in carcerand-like containers is based on the formation of kinetically stable host-guest complexes. All the examples discussed above share in common that the reactive species were generated in the inner cavity of the molecular container from a stable precursor previously encapsulated using constrictive binding. Thus, the *in situ* produced reactive species was stabilized and spectroscopically detected and characterized. This approach was useful for the detection of short-lived reaction intermediates that assisted the elucidation of complicate reaction mechanisms.

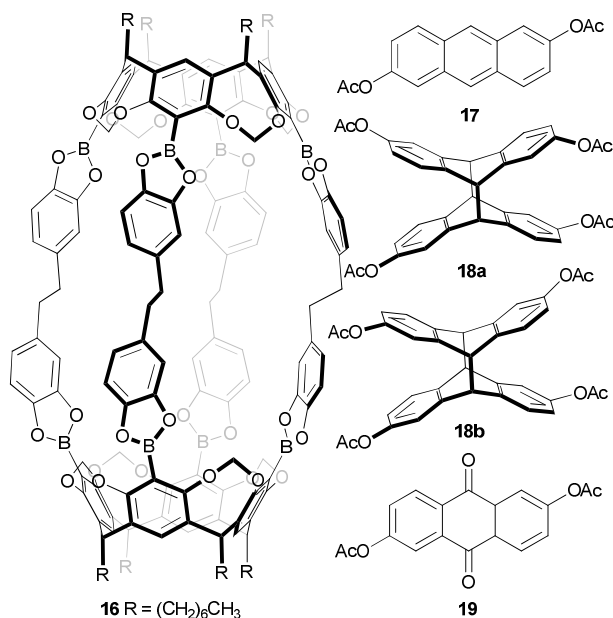


**Figure 5.** Line-drawing structures of the capsule and the molecules described in Kobayashi's work.

A quite different scenario was reported several years later. Kobayashi et al. exploited the reversibility and strength of dynamic boronic ester bonds to assemble a covalent capsule having two hemispheres based on a resorcin[4]arene caviting scaffold. A molecule of 2,6-diacetoxyanthracene (**17**) was reversibly encapsulated within container **16** (Figure 5).<sup>62</sup> Irradiation of C<sub>6</sub>D<sub>6</sub> solutions of **17** with 365 nm light produced the photodimerization and the photooxygenation by-products **18** and **19**, respectively, within one hour. In contrast, light irradiation of solutions of capsule **17@16** (Figure 6) did not induce the formation of any of the two by-products even after 2 hours.

The confined space within the capsule **16** did not allow the inclusion of two molecules of **17** avoiding its dimerization reaction yielding **18**. The authors proposed that the absence of the photooxygenation by-product **19** was due to a high energy transition state of the photooxygenation reaction occurring within the capsule. Even if oxygen was able to pass through the portals of **16**, the conversion of **17** into **19** required a bent transition state that would be highly costly energetically within the constricted space of the cavity. This example differs significantly from those reported by Cram and Warmuth, which were discussed above. Here, the encapsulation process protects the short-lived diradical species generated "*in situ*" to react further but it was not used for its characterization.

In the following sections, we will encounter examples of reactive species stabilization that rely on sequestering them from the bulk and not in their "*in situ*" generation from an encapsulated precursor as we have described so far.

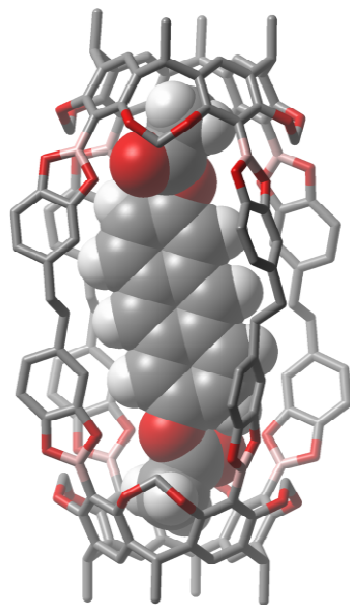


**Figure 6.** Energy-minimized (MM3) structure of the 17C16 complex. The host is depicted in stick representation and the guest as CPK.

#### Molecular containers with covalent structure and functionalized cavities

The examples discussed above are solid contributions to the field of molecular encapsulation and began to exploit the possible applications of molecular containers. However, the lack of functionalization of the aromatic cavities limited the scope of guest encapsulation and often compromised the affinity and selectivity of the encapsulation complexes. More recently other groups have designed molecular containers with covalent structure and inner cavities decorated with polar groups that are able to establish directional interactions with the bound guests. Recently, it was reported that the organic receptor **20** (Figure 7a) was able to encapsulate and stabilize methyl iodide.<sup>63</sup> Methyl iodide (a.k.a. iodomethane, MeI) is a volatile and very electrophilic reagent, widely used in organic synthesis as a source of methyl groups.

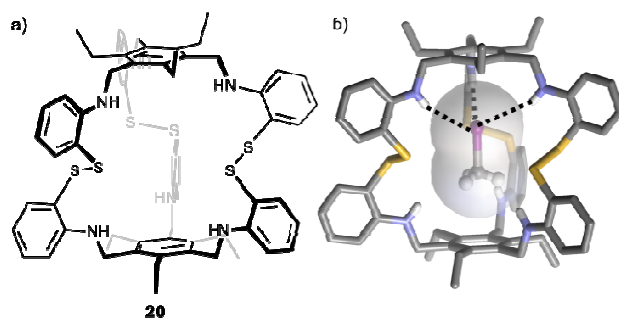


**Figure 7.** a) Line-drawing structure of receptor **20**. b) X-ray structure of the MeI-**20** complex. Non-polar hydrogen atoms of the host are removed for clarity. NH...I interactions are marked with dashed lines.

However, the design of receptors that selectively encapsulate and store methyl iodide is challenging because of the potential

threat of self-methylation of the container. In the presence of methyl iodide, receptor **20** formed a 1:1 inclusion complex without undergoing self-methylation of the receptor. Iodomethane dissolved in toluene evaporated completely within a week, however it remained in solution at least for four months under ambient conditions when encapsulated in **20**. At 80 °C bound iodomethane was released from the cavity and vaporized. The solid-state structure of the MeI-**20** complex revealed that the bound iodomethane formed three NH...I hydrogen-bonding interactions with the NHs of three amine groups of the receptor (Figure 7b). In addition, a weak lp- $\pi$  interaction was detected between the lone electron pairs of the iodide atom and one of the triethyl phenyl spacers of the receptor.

Other iodoalkanes (i.e. EtI, <sup>i</sup>PrI) were not encapsulated within receptor **20**. The calculated packing coefficient values (PC) for the series of encapsulation complexes shed some light about the selective inclusion of MeI with respect to the larger iodoalkanes (PC: 0.57 for MeI-**20**; for EtI or <sup>i</sup>PrI complexes the PCs: > 0.75). The authors claimed that the combination of conformational rigidity of the receptor with the complementarity of binding sites for the iodide atom and host-guest volumes matching were responsible of the selective inclusion and stabilization of methyl iodide in **20**. It is worth noting that cage **20** stabilized MeI by direct encapsulation of the reactive species.

Zhao and Wang reported the formation of supramolecular complexes between the azacalix[6]pyridine scaffold **21** (Figure 8a) and a reactive silver carbide cluster.<sup>64</sup>

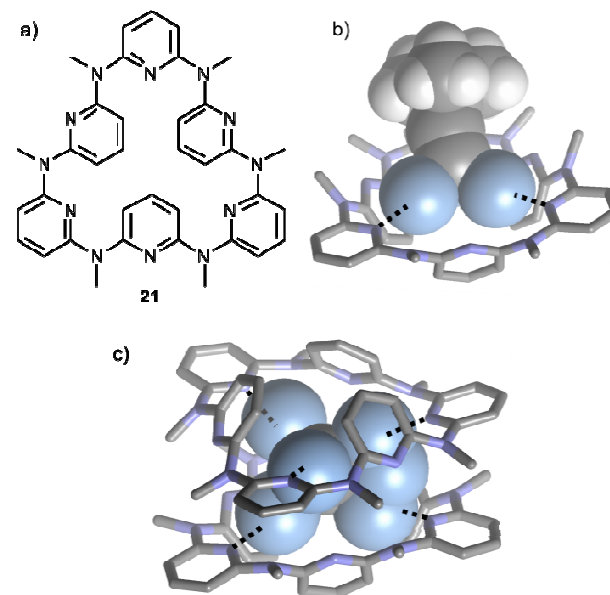
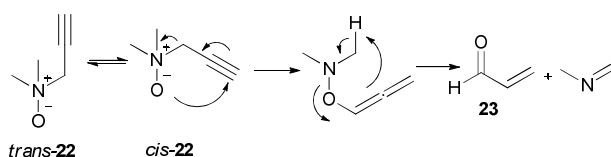


**Figure 8.** a) Line-drawing structure of azacalix[6]pyridine **21** and X-ray structures of the silver carbide clusters stabilized by ligand **21** prepared with b) *tert*-butyl acetylene c) *tert*-butyl acetylene. Hydrogen atoms of the host, triflate ions, solvent molecules and silver atoms of the cluster non-coordinated to the alkyne are removed for clarity. The host is depicted in stick representation and silver carbide cluster shown as CPK model. N...Ag coordination bonds marked with dashed lines.

Silver carbides are highly explosive and very sensitive to heating or mechanical shock but upon complexation they could be isolated and characterized even in the solid-state. Three different polynuclear silver carbide clusters were prepared, isolated and characterized by X-ray diffraction analysis. On the one hand, the combination of ligand **21** (Py6) with silver triflate and *tert*-butylacetylene produced the formation of a silver carbide cluster in which the *tert*-butylacetylide silver cluster was positioned in the middle of the bowl-cavity of **21** (Figure 8b).

The silver atoms of the acetylide group were coordinated to the nitrogen atoms of three alternating pyridine units of the Py6 ligand scaffold. On the other hand, the use of ditopic acetylenic ligands i.e. (1,3-butadiyne, acetylene) afforded supramolecular clam-like structures (Figure 8c). The bis-multinuclear silver acetylide cluster was sandwiched between two units of **21** and formed a total of six Ag-N coordination bonds. Each Py6 ligand of the dimer formed three coordination bonds between its alternating pyridine nitrogen atoms and the terminal trinuclear silver clusters of the bis-silver acetylide. In this case, the reactive species (polynuclear cluster) is generated “*in situ*” by the formation of non-covalent Ag-N coordination bonds with the organic scaffold Py6. Later on, we will discuss related examples in which the inner cavity of the container magnifies the formation and stabilization of highly reactive species, the so-called cavity-directed synthesis.

We reported the stabilization of the reactive *N,N*-dimethyl-2-propyn-1-amine *N*-oxide **22** by encapsulation in two different containers based on a calix[4]pyrrole scaffold.<sup>65</sup> Tertiary propargylamine *N*-oxides experience a concerted [2,3]-sigmatropic rearrangement followed by a rapid elimination generating propenal (**23**) and an imine (Scheme 1).<sup>66,67</sup> We envisaged that the inclusion/encapsulation of the *N*-oxide **22** in a molecular container that energetically and/or sterically disfavored its *cis*-conformation would stabilize it. The *N*-oxide **22** must adopt the *cis*-conformation to achieve the transition state of the sigmatropic rearrangement that produces its decomposition.



**Scheme 1.** Reaction pathway for the decomposition of *N*-oxide **22** into propenal (**23**).

We selected as molecular container an aryl-extended “four-wall” calix[4]pyrrole receptor. The inclusion of **22** in cavity’s container must be driven by the formation of four convergent hydrogen bonds between the oxygen atom the *N*-oxide group and the pyrrole NHs of the calixpyrrole core. These interactions should reduce significantly the nucleophilicity of the oxygen atom of the *N*-oxide. Moreover, molecular modelling studies indicated the existence of strong steric clashes between the aromatic walls of the receptor and the

propynyl residue of the included **22** in *cis*-conformation. Taken together, these considerations were promising starting points for the stabilization of **22**.

The decomposition of a CD<sub>2</sub>Cl<sub>2</sub> solution of **22** was monitored by <sup>1</sup>H NMR spectroscopy. The kinetic data nicely fit to a first-order reaction. After 13 hours, the *N*-oxide **22** was almost fully converted into propenal. From the fit of the kinetic data to the theoretical model, we determined a rate constant value of  $k = 5.0 \pm 0.3 \times 10^{-5} \text{ s}^{-1}$  ( $t_{1/2} = 3.8 \pm 0.2 \text{ h}$ ) for the decomposition reaction of *N*-oxide **22** free in solution into propenal **23**. Molecular modelling studies indicated that the deep and polar aromatic cavity provided by calixpyrrole **24** in cone conformation (Figure 9a) was a good fit for the *trans*-conformation of the *N*-oxide **22** (Figure 9c). On the contrary, and as already mentioned above, the *N*-oxide **22** in the *cis*-conformation did not match in terms of size and shape with the receptor’s cavity. In the presence of 1 equivalent of aryl-extended calixpyrrole **24**, the stability of **22** in solution was increased almost 18-fold ( $t_{1/2} > 50 \text{ h}$ ).

We deduced a mathematical model that related the thermodynamic stability of the inclusion complexes to the observed kinetic stability of the *N*-oxide **22**. In fact, when the *N*-oxide **22** was co-encapsulated with a molecule of CDCl<sub>3</sub> within the cavity of bis[2]catenane **25** (Figure 9b), we did not observe the presence of the signals corresponding to the protons of propenal in the <sup>1</sup>H NMR spectra of the mixture that were acquired regularly during a period of time of two months.

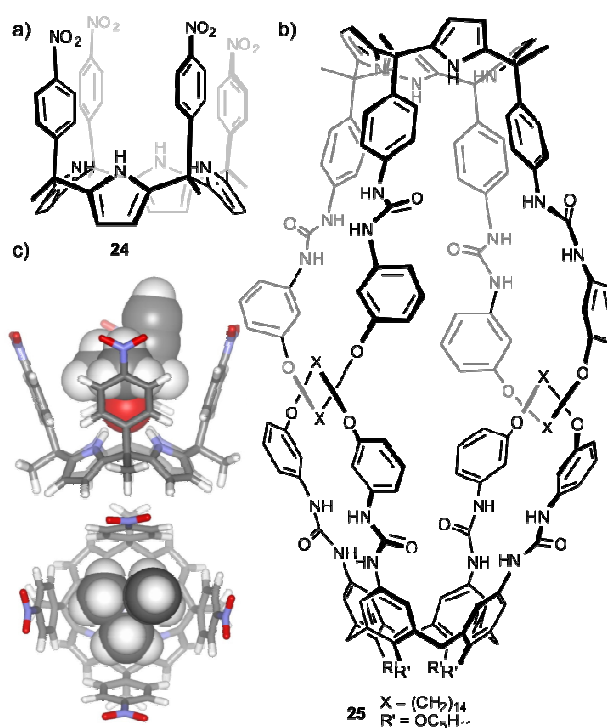


**Figure 9.** a,b) Line-drawing structures of receptors **24** and **25**. Both receptors have molecular structures based on a calixpyrrole scaffolds. c) Top and side views of the energy-minimized (MM3) structure for the *cis*-**22** complex.

The developed mathematical model predicted that the stability constant of the **22**⊂**25** encapsulation complex should be more than two orders of magnitude larger than that of the inclusion complex **22**⊂**24**.

The results obtained in isothermal titration calorimetry (ITC) experiments provided full experimental support to this prediction. The developed mathematical model supported that the observed kinetic stabilization of the *N*-oxide resulted from the significant reduction of free **22** in solution when 1 equivalent of container **25** was added. The rate constant for the release of encapsulated **22** to the bulk solution was not the rate-limiting step in the decomposition process of **22**. This work constituted a remarkable example of direct encapsulation of a reactive guest. Such methodology could be applied in the safe storage of very reactive or volatile substances that could be released at will by binding of a competitive guest.

### Stabilization of reactive species within self-assembled containers

Self-assembled containers rely on the use of non-covalent interactions (i.e. metal-ligand or hydrogen bonding interactions) for their stabilization and from a synthetic viewpoint are more interesting than their covalent counterparts. Starting from a reduced number of simple building blocks and exploiting the reversibility of the non-covalent interactions, complex supramolecular architectures have been efficiently assembled. In the next section, we will discuss relevant examples of stabilization of reactive species within self-assembled containers.

#### Coordination cages based on metal-ligand bonds

Fujita and co-workers reported the preparation of water-soluble coordination cages (**26**, Figure 10) able to bind strongly a variety of neutral guests mainly through hydrophobic interactions.<sup>68</sup> Cage **26a** was shown to readily encapsulate 3 to 4 molecules of trisilanol **27a**.<sup>69</sup> Trisilanols are very reactive species that quickly polycondensate to form siloxane networks.

Cyclic trimers **28** were considered to be short-lived intermediates in the polycondensation of trisilanols and they had never been isolated in a pure or stable form. Once formed, the cyclic trimers were rapidly converted to cyclic tetramers and further condensation products. However, in aqueous solution the encapsulation complex (**27a**)<sub>n</sub>⊂**26a** (*n* = 3–4) was converted within one hour into a new encapsulation assembly **28a**⊂**26a**. Control experiments indicated that the formation of the cyclic trimer occurred within the cavity's cage through a *ship-in-a-bottle* mechanism. Although the small trisilanol monomers can enter and exit the supramolecular container, once the cyclic trimer is formed within the cavity of the cage it cannot escape owing to its larger dimensions. Analogous results were obtained when the sterically more crowded trisilanol **27b** was used affording the final encapsulation assembly **28b**⊂**26a**. Interestingly, the bulky cyclic trimer **28b**

experienced restricted motions within the cage reducing its symmetry from tetrahedral to *C*<sub>3</sub>. Cyclic trimers (i.e. **28a**, **28b**) were stabilized within the cage adopting an all-*cis* conformation (Figure 11). The structure of the encapsulated trimer **28b** remained intact after a month in aqueous solution at room temperature. Even in acidic media (pH < 1) the encapsulated trimer **28b** was unaltered.

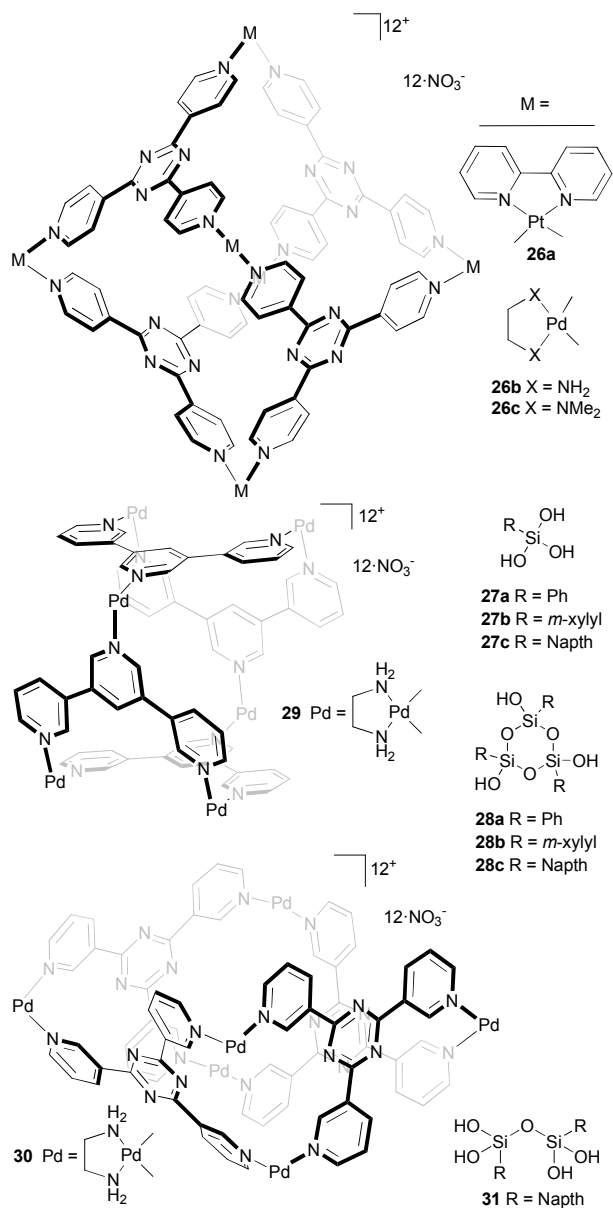
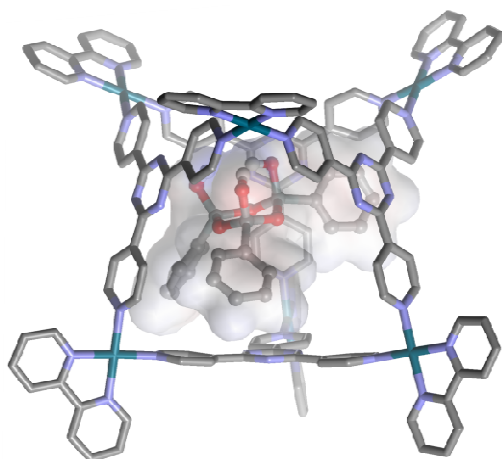


Figure 10. a) Line-drawing structures of the coordination cages **26**, **29** and **30** reported by Fujita, trisilanols **27** and the cyclic trimers **28**.

The ship-in-a-bottle synthesis of siloxane cyclic trimers was further elaborated into a general concept of cavity-directed synthesis.<sup>70</sup> Trisilanol **27c** was encapsulated in three different containers (**29**, **30** and **26b**; Figure 10). Different labile siloxane

oligomers were also formed and stabilized depending on the cavity size of each container.



**Figure 11.** Energy-minimized (MM3) structure of the **28b**–**26a** encapsulation complex. Non-polar hydrogen atoms and nitrate anions were removed for clarity.

The reduced dimensions of the cavity in cage **29** allowed for the encapsulation of just one molecule of trisilanol **27c** and precluded further condensation. Complex **27c**–**29** was stable in aqueous solution for one week at 80 °C and its structure was characterized in the solid-state. The analysis of the X-ray structure revealed the existence of  $\pi$ – $\pi$  and CH– $\pi$  interactions between the naphthyl group of the trisilanol and the aromatic rings of the cage (Figure 12a). The reactive Si(OH)<sub>3</sub> knob is not involved in any intermolecular interactions but it is shielded from the bulk solvent. Conversely, the larger bowl-shaped cavity of cage **30** can incorporate two molecules of trisilanol **27c** in its interior. As expected, an aqueous solution of trisilanol **27c** and cage **30** resulted in the rapid formation of the encapsulation complex **31**–**30** comprising one unit of a labile siloxane dimer. The solid state structure of the complex revealed that the bound dimer was strongly folded due to the  $\pi$ – $\pi$  interactions that existed between its naphthyl groups and the cage's aromatic walls (Figure 12b). In the free state, cage **30** adopted a conformation providing a bowl-shaped structure to its aromatic cavity.<sup>71</sup> However, to better accommodate the included guest bound cage **30** experienced a conformational change giving rise to an aromatic cavity with box-like structure. In solution, the two conformers were in a chemical exchange process that was intermediate on the NMR timescale.

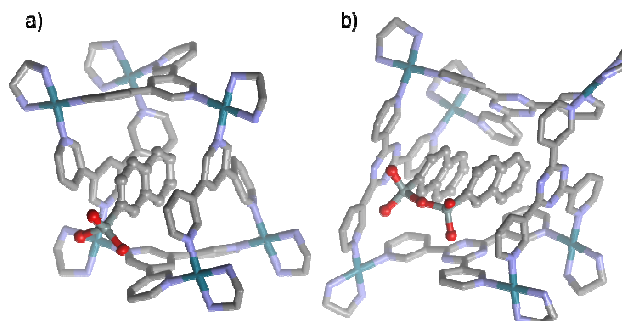


**Figure 12.** X-ray structures of the complexes a) **27c**–**29** and b) **31**–**30**. Hydrogen atoms, nitrate anions and water molecules were removed for clarity.

Tetrahedral cage **26b** stabilized a cyclic trimer of siloxanes in similar fashion to what we discussed above for the structurally analogous counterpart **26a**. The cavity size of **26b** allowed the inclusion of three molecules of trisilanol **27c**. Thus, the resulting encapsulation complex **28c**–**26b** was readily formed in aqueous solution. Its structure was fully characterized in the solid-state. In the solid state, the bound trimer **28c** adopted an all-*cis* conformation that was analogous to the one observed for the bound trimer in the **28b**–**26a** encapsulation complex (Figure 11).<sup>72</sup>

Taking advantage of the relatively large cavity featured by cage **26b**, Fujita and co-workers prepared the encapsulation complex **32**<sub>4</sub>–**26b** in aqueous solution. In this complex, four copies of the organometallic complex methylcyclopentadienyl manganese tricarbonyl (**32**, MCMT, Figure 13) were loosely comprised within the hydrophobic cavity defined by the aromatic walls of the cage.<sup>73</sup> Interestingly, photoirradiation of a single crystal of the complex **32**<sub>4</sub>–**26b** at 100K allowed the direct crystallographic determination of a coordinatively unsaturated manganese complex. Prior to this finding, such labile unsaturated transition metal complexes had been detected only by spectroscopic methods. The spectroscopic observation had generated strong discussions on the geometry adopted by these transient intermediates.<sup>74</sup> After photoirradiation of the **32**<sub>4</sub>–**26b** crystal, one CO ligand was dissociated from one of the bound Mn organometallic complexes **32** without significant loss of crystallinity. The CO was trapped in the voids of the packing of the crystal and the structure of the resulting 16-electron unsaturated manganese complex **33** could be solved by analysis of the X-ray diffraction data (Figure 13).

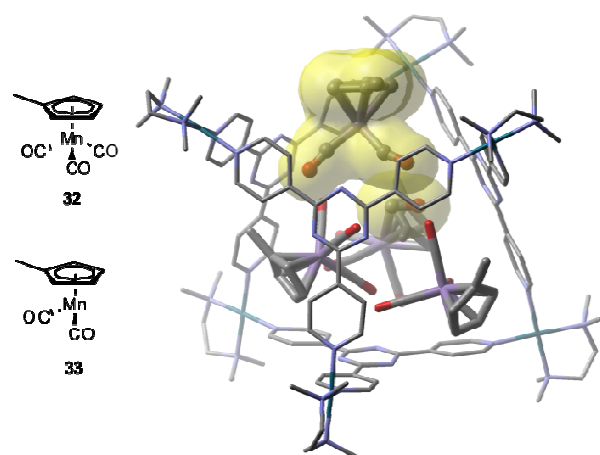


**Figure 13.** Line-drawing structures of the manganese transition-metal complexes **32** and **33** and X-ray structure of the  $(\mathbf{32}_2\mathbf{33}_2\cdot\text{CO})_2\mathbf{26b}$  encapsulation complex. Hydrogen atoms, solvent molecules and nitrate anions were removed for clarity. Bound **33** and CO are shown with a yellow transparent van der Waals surface.

The released CO ligand was separated more than  $3\text{ \AA}$  from bound **33**, avoiding recombination with the metal center. Only one of the four molecules of bound **32** was selectively converted to **33** because the crystalline packing could not incorporate more than one CO molecule per cage. Bound **33** was observed to adopt a pyramidal geometry, settling the discussion about the geometry of these labile species. Once more, it was proved that the tight binding experimented by the guests within the cage was responsible for the stabilization of otherwise very reactive species. This example can be related to the early examples of Cram and Warmuth where the reactive species was generated by reaction of a previously encapsulated stable precursor.

Fujita also described the stabilization of a dinuclear ruthenium complex by supramolecular inclusion in a tetrahedral palladium cage.<sup>75</sup> Organometallic complex **34** (Figure 14a) exists as a mixture of *cis* and *trans* bridged and non-bridged isomers that are in equilibrium in solution. Nevertheless, only the *trans* isomer had been observed in the solid-state. In addition, dinuclear complex **34** is photosensitive: within a few days under room light the Ru-Ru bond rapidly cleaves and CO ligands dissociate. Fujita described the supramolecular inclusion of complex **34** within coordination cage **26c** (Figure 10a). Interestingly, in the solid-state complex **34** $\subset$ **26c** showed bound **34** in a *cis*-conformation (Figure 14b). Even if the *cis*-to-*trans* equilibrium required small structural changes, the tight confinement in the cage avoided this transition. Complex **35**, sterically less demanding, was also included within the cavity of cage **26c** in a *cis* conformation. However, in this case due to the less tight host-guest fit, rapid exchange between terminal and bridged CO ligands was observed. In addition, the complex *cis*-**34** $\subset$ **26c** was protected towards photodecomposition, and the encapsulated organometallic ruthenium complex remained intact in solution for several months.

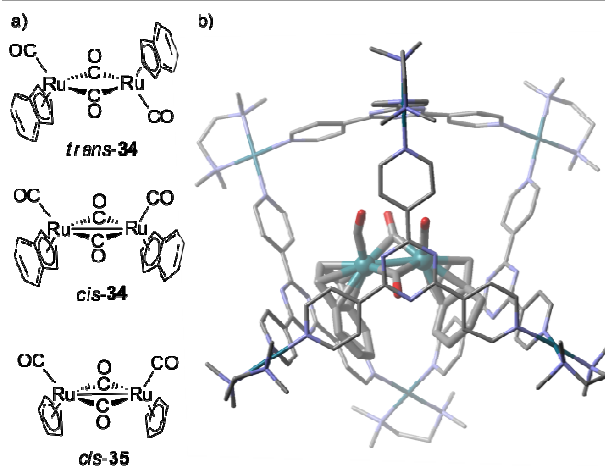


**Figure 14.** a) Line-drawing structures of the organometallic ruthenium complexes used by Fujita. b) X-ray structure of the complex *cis*-**34** $\subset$ **26c**. Hydrogen atoms were removed for clarity. The host is depicted in line representation and the guest in stick representation.

Raymond et al. also explored the stabilization of reactive organometallic species by supramolecular encapsulation in coordination cages.<sup>76</sup> They reported the preparation of self-assembled water-soluble cages comprised by six bidentate catecholamide ligands and four metal centers bridged in a tetrahedral fashion (**36**, Figure 15a).<sup>77</sup>

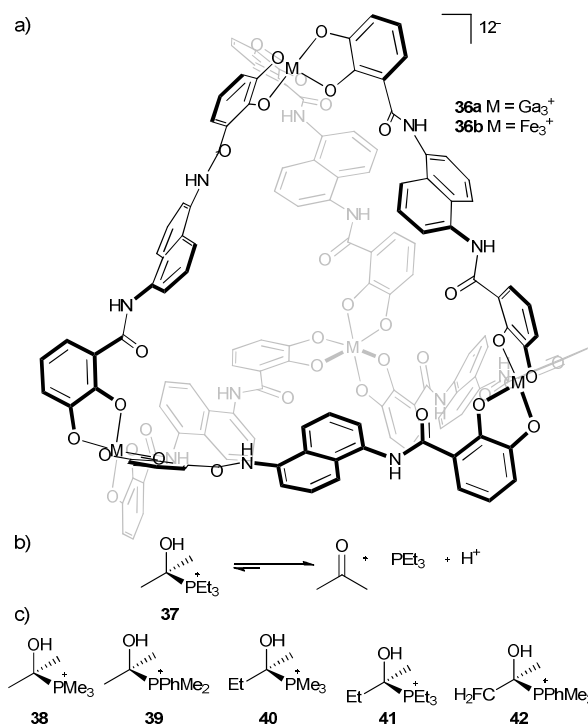


**Figure 15.** a) Schematic and line-drawing structures of the tetrahedral cages **36** reported by Raymond et al. b) Decomposition reaction of phosphine-acetone adduct **37**. c) Line-drawing structures of other labile cationic adducts.

Tetrahedral cage **36** was able to encapsulate cationic species with high affinity (e.g. tetraethylammonium) in aqueous solutions.<sup>77</sup>

Phosphine-acetone adduct **37** has been prepared and isolated in anhydrous solutions, but in the presence of water the adduct rapidly reverted to the initial acetone and phosphine (Figure 15b). Surprisingly, addition of triethylphosphine to an aqueous solution of cage **36a** resulted in the rapid formation of an encapsulation complex **37**⊂**36a**. Cage **36a** had embedded acetone molecules that derived from the use of this solvent in the precipitation process required for its isolation. The addition of triethylphosphine resulted in the formation of the adduct **37** that appeared encapsulated. The exclusion of water molecules from the hydrophobic interior of cage **36a** provoked the stabilization of the bound adduct **37** for several hours in D<sub>2</sub>O and at least one day in methanol-*d*<sub>4</sub>. Initially, the authors proposed that the formation of the reactive adduct occurred inside the cavity. These interesting results prompted a more thorough study of the stabilization of cationic species within the cavity of tetrahedral coordination cages.<sup>78</sup> An aqueous solution of cage **36a**, prepared avoiding the use of acetone, produced the encapsulation complex HPEt<sub>3</sub><sup>+</sup>⊂**36a** upon addition of triethylphosphine. The addition of acetone to the previously formed HPEt<sub>3</sub><sup>+</sup>⊂**36a** encapsulation complex resulted in the observation of the **37**⊂**36a** complex. Unfortunately, the obtained results did not clarify if the phosphine-acetone adduct was formed within the cavity of the cage or in the bulk solution prior to being encapsulated. The equilibrium shown in Figure 15b indicates that in acid conditions the amount of the phosphine-acetone adduct in solution increases. The authors described that lowering the pD values increased the percentage of the **37**⊂**36a** complex observed in solution. In turn, the diminution of the amount of phosphine free in solution slowed down its degradation and extended the lifetime of the encapsulation complex. When the pD was adjusted to ca. 5.2 the **37**⊂**36a** complex was stable for two days in aqueous solution, compared to just 6 h at pD = 8.

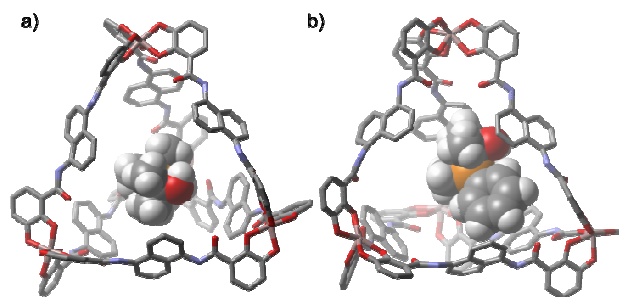


**Figure 16.** Energy-minimized (MM3) structures of the encapsulation complexes a) **38**⊂**36a** and b) **39**⊂**36a**. Hydrogen atoms of the host (stick representation) were removed for clarity. Guests shown as CPK models.

Larger phosphines (i.e. PPh<sub>2</sub>Me) did not form acetone adducts that were encapsulated. Conversely, PMe<sub>3</sub> and PPhMe<sub>2</sub> formed acetone-adducts **38** and **39**, respectively (Figure 15c) that were detected as species included in the cage. Encapsulation complexes **38**⊂**36a** (Figure 16a) and **39**⊂**36a**

(Figure 16b) were stable in D<sub>2</sub>O for several days (pD ~ 5.2). The encapsulation complex **38**⊂**36a** was completely formed within minutes. On the contrary the formation of the complex **39**⊂**36a** that contained the larger cationic adduct **39** took nearly 30 minutes.

It is worthy to mention that cage **36** existed as a mixture of two enantiomers (ΔΔΔΔ or ΛΛΛΛ depending on the orientation of the octahedral propeller-like of the metal vertices). The encapsulation of a chiral guest afforded two enantiomeric pairs of diastereoisomeric complexes that were distinguishable by NMR. The replacement of acetone by butanone or fluoroacetone afforded chiral adducts (**40**–**42**, Figure 15c) in racemic form. The two enantiomers of adducts **40**–**42** were readily encapsulated within the cavity of **36a** but in different extents. The authors observed that larger adducts induced higher levels of diastereoselectivity in their encapsulation process. This result was rationalized considering that steric contacts between the chiral guest and the chiral cavity increased with the size of former. For instance, the formation of the encapsulation complex **42**⊂**36a** occurred with a diastereomeric excess (*de*) of 38% but only a 28% *de* was measured for the formation of the **41**⊂**36a** complex. Finally, the formation of the **40**⊂**36a** complex showed no preference for the encapsulation of any of the two enantiomers of the guest. The encapsulation complexes formed with the butanone adducts were more stable kinetically than those formed using acetone: complex **40**⊂**36a** persisted in aqueous solution for more than three weeks. Conversely, the presence of fluorine atoms in the ketone-adducts rendered the corresponding encapsulation complex kinetically less stable.

In a similar manner, Bergman and Raymond exploited the hydrophobic nature cage's **36a** cavity to stabilize iminium ions in water.<sup>79</sup> Iminium ions are reversibly formed by the condensation reaction of ketones with amines (Figure 17a). However, in water this equilibrium is shifted towards the starting reactants and the iminium ions exist only as transient species. Nevertheless, an aqueous solution of an amine and ketone in the presence of cage **36a** showed a <sup>1</sup>H NMR spectrum with the expected earmarks of an encapsulation complex comprising the encapsulated iminium ion. The transient cationic iminium ions formed in solution were readily encapsulated and stabilized in the hydrophobic cavity of the cage, shifting the equilibrium shown in Figure 17a towards the products. The size of both the amine and the ketone played a key role for the efficient formation of encapsulation complexes with the corresponding iminium ions. An aqueous solution of cage **36a** produced the encapsulation complex **43**⊂**36a**. The encapsulated iminium **43** (Figure 17b) was stabilized for months at room temperature in water, even at basic pH. Similar results were obtained by combining pyrrolidine and 3-hexanone affording the iminium encapsulation complex **44**⊂**36a** (Figure 17c). In both cases, the alkyl chain adopted a fully extended conformation to minimize *gauche* interactions. Iminium ions with larger alkyl must coil to fit within the cavity boundaries. Interestingly, the iminium ion **45** resulting from

the condensation reaction of pyrrolidine and 2-undecanone was not encapsulated in the cavity of **36**. Iminium **45** possesses a large alkyl chain that even coiled or folded could not be accommodated in the cavity dimensions of the cage. The formation of encapsulation complexes with the coordination cages not only required that the guests were positively charged and somewhat hydrophobic but also they must be complementary fit in terms of size and shape with the cavity. Competitive experiments performed between amines and ketones of different sizes highlighted the importance of the fit between host and guest and revealed the ability of the cage to recognize small structural variations of the guests. The stabilization of cationic species (both phosphine-acetone adducts and iminium ions) can be considered to be akin to the cavity-directed synthesis of reactive silanols.

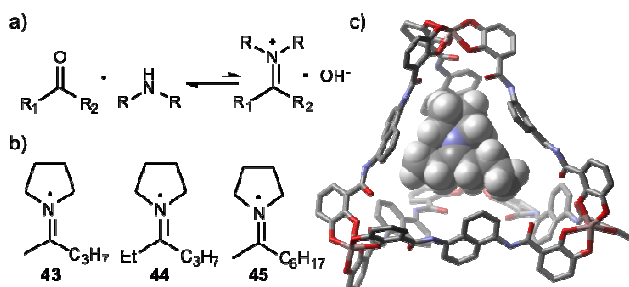


**Figure 17.** a) Reaction scheme of the formation of iminium ions. b) Line-drawing structure of iminium ions used. c) Energy-minimized (MM3) structure of the encapsulation complex **44**⊂**36a**. Hydrogen atoms of the host (stick representation) removed for clarity. Guest shown as CPK model.

The hydrophobic interior of cage **36a** was also used for the encapsulation and stabilization of reactive aromatic ions.<sup>80</sup> Diazonium and tropylium cations are reactive aromatic compounds that decompose in aqueous solution in less than one day.

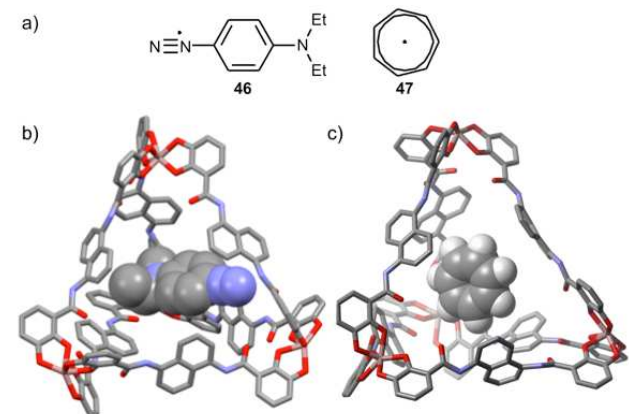


**Figure 18.** a) Line-drawing structures of the aromatic cations **46** and **47**. Energy-minimized (MM3) structures of the encapsulation complexes b) **46**⊂**36a** and c) **47**⊂**36a**.

Cation **46**, as tetrafluoroborate salt, (Figure 18a) was readily encapsulated in cage **36a**. The encapsulation complex

persisted for five days (Figure 18b). Hydrophobic interactions, as well as van der Waals forces between the ethyl groups of the guest and the aromatic walls of the cage contributed to the thermodynamic stabilization of the complex. Likewise, cation **47** as tetrafluoroborate salt persisted in the interior of cage **36a** for at least 20 hours (Figure 18c).

Raymond and Bergman have also reported the stabilization of reactive organometallic species by inclusion in tetrahedral coordination cages. Ruthenium complex **48** was encapsulated in cage **36b** (Figure 19a and Figure 15).<sup>15</sup> The tetrafluoroborate salt of cation **48** decomposes quickly in the presence of water to form the complex [CpRu(1,3,5-cyclooctatriene)]BF<sub>4</sub> (**49**) with concomitant release of hydrogen. Conversely, the complex **48**⊂**36b** (Figure 19b) was stable in water for several weeks at room temperature.

The encapsulated organometallic Ru complex **48** was sheltered from the bulk and protected towards possible decomposition pathways when encapsulated in **36b**, but it was not completely inert. Thus, exposure of the **48**⊂**36b** complex to CO produced the new encapsulation complex **50**⊂**36b**. Most likely, the coordination of the CO ligand to the Ru center occurred within the cavity due to the small size of the ligand.

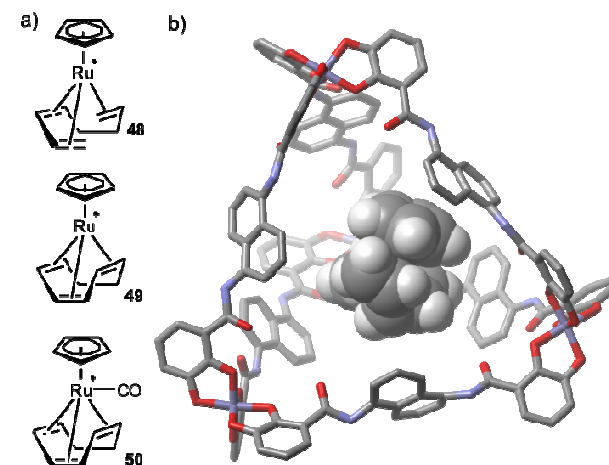


**Figure 19.** a) Line-drawing structures of the organometallic compounds **48**, **49** and **50** b) Energy-minimized (MM3) structure of the **48**⊂**36b** encapsulation complex. Hydrogen atoms of the host (stick representation) were removed for clarity. Guest **48** is shown as CPK model.

Nitschke took advantage of the tight and hydrophobic microenvironment provided by an unprecedented self-assembled coordination cage **51** to stabilize pyrophoric white phosphorus, P<sub>4</sub>.<sup>81</sup> Cage **51** (Figure 20a) quantitatively formed an encapsulation complex with P<sub>4</sub> in aqueous solution. The complex P<sub>4</sub>⊂**51** was air-stable for four months and its structure was characterized by X-ray diffraction (Figure 20b). The solid state structure of the complex revealed the existence of van der Waals interactions between the bound guest and the aromatic phenylene groups of the cage that contributed to its overall stabilization. The openings of the cage are wide enough to allow the entering of O<sub>2</sub>. The authors proposed that the

stabilization of  $P_4$  resulted from the tight and constrictive binding provided by the cage's cavity. In other words, the oxidation products could not fit within the cavity of cage **51** and provoked that the decomposition reaction should take place through a very high energy transition state.

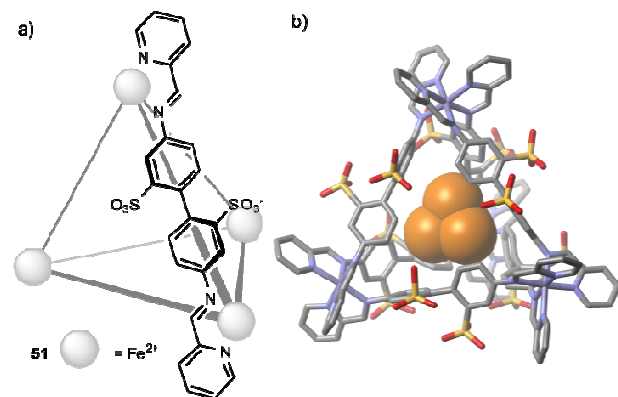


**Figure 20.** a) Line-drawing structure of tetrahedral cage **51** reported by Nitschke. b) X-ray structure of the complex  $P_4@51$ . Hydrogen atoms, solvent molecules and counterions were removed for clarity.

The bound phosphorous  $P_4$  was released by the addition of a competitive guest such as benzene or cyclohexane. These guests are good fits for the cavity of the cage and also solubilize the released  $P_4$ . In contrast, the addition of heptane to an aqueous  $P_4@51$  solution did not extract the encapsulated guest. Although the phosphorus was soluble in heptane, owing to its large size this solvent was not a good fit for the cage's cavity. The organic solutions containing the extracted white phosphorus rapidly decomposed when exposed to air.

Recently, Yoshizawa reported the stabilization of radical initiators such as azobisisobutyronitrile (AIBN) by supramolecular encapsulation into a polyaromatic metallo-cage.<sup>82</sup> Radical initiators such as AIBN or its derivatives are light, heat and shock sensitive. The authors envisaged that the encapsulation of such species within the cavity of a hydrophobic cage based on fused aromatic rings that could absorb photons would render more stable the radical initiators. A 9:1  $D_2O/CD_3CN$  solution of cage **52** quantitatively formed the inclusion complex **53** $\subset$ **52** in the presence of equimolar amounts of AIBN at millimolar concentration (Figure 21a). The structure of the complex was characterized in the solid-state (Figure 21b) showing that the encapsulated AIBN adopted an S-shaped *trans* configuration. The complex was stabilized by weak intermolecular interactions between the nitrile groups of the guest and the palladium centers of the cage. UV light irradiation of an aqueous solution of the **53** $\subset$ **52** complex for 10 hours at room temperature did not decompose the radical initiator. Conversely, a solution of free **53** exposed to similar irradiation conditions yielded exclusively decomposition products. The half-lives estimated for the free and bound AIBN were 1.8 and 690 hours respectively, indicating that the bound radical initiator was 380-fold more stable than free. A similar result was obtained with the

analogous AMBN (**54**), which was 580-fold more stable when bound within cage **52**. Larger AMMVN (**55**) was also stabilized against light ca. 50-fold.

Encapsulation complexes **53** $\subset$ **52** and **54** $\subset$ **52** did not show evidence of thermal stabilization. Unexpectedly, bound **55** showed an unusual increased stability towards heat. A  $D_2O/CD_3CN$  solution of **55** $\subset$ **52** was stable for several weeks at room temperature and ten hours at 50 °C whereas a solution of free **55** decomposed rapidly at 50 °C ( $t_{1/2} = 1.1$  h). The authors attributed these results to the tight fit that existed between the larger guest **55** and the cavity of cage **52**. AMMVN **55** must adopt a C-shaped conformation in order to fit within the cage's cavity. The stabilization of light sensitive radical initiators by encapsulation in cage **52** is an analogous to example reported by Kobayashi and discussed above (Figure 5).

It is interesting to note that the last commented examples (encapsulation of tropylium and diazonium cations, Ru-complex **48**, white phosphorus and radical initiators) rely on the stabilization of the reactive guests by their direct encapsulation in the molecular container.

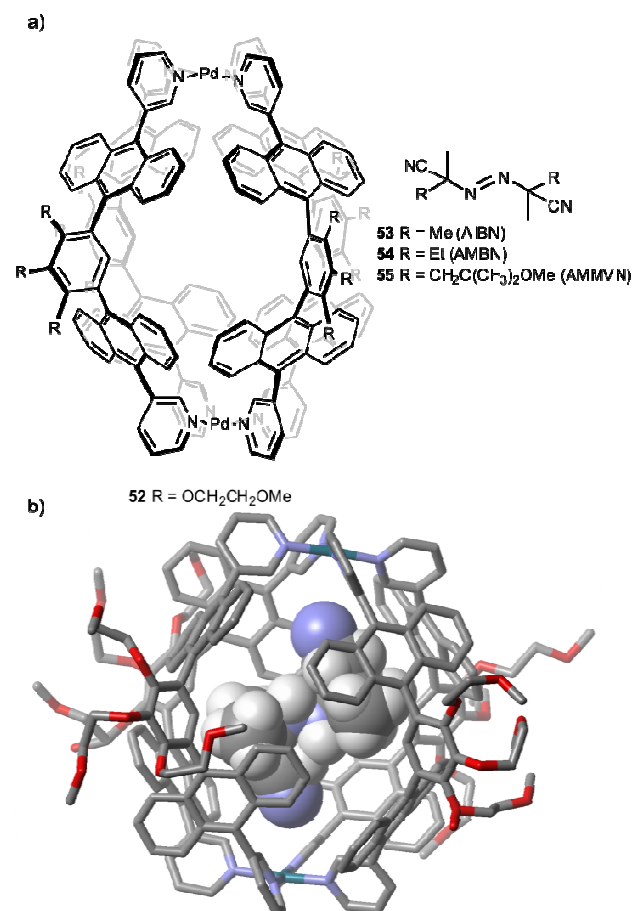


**Figure 21.** a) Line-drawing structures of cage **52** and radical initiators **53**–**55**. b) X-ray structure of the **53** $\subset$ **52** complex. Hydrogen atoms of the host (stick representation) and water molecules were removed for clarity. The encapsulated guest is shown as CPK model.

### Hydrogen bonded capsules

Rebek described the preparation of self-assembled dimeric capsule **56**<sub>2</sub>. Typically, in non-polar solvents and in the presence of suitable guests the imide groups installed at the upper rim of cavitand **56** (Figure 22a) held together the two cavitand units of the dimer by forming an array of 16 intermolecular hydrogen bonds.<sup>83</sup> Mesitylene-*d*<sub>12</sub> is not suitable to induce the assembly of the dimer owing to a reduced size and shape complementary with the capsule's internal volume. Using this solvent, Rebek et al. found that benzoyl peroxide **57** was readily encapsulated in the dimer **56**<sub>2</sub>.<sup>84</sup> Benzoyl peroxide was indeed a perfect complementary fit in terms of size and shape to the inner cavity of **56**<sub>2</sub> (Figure 22b).

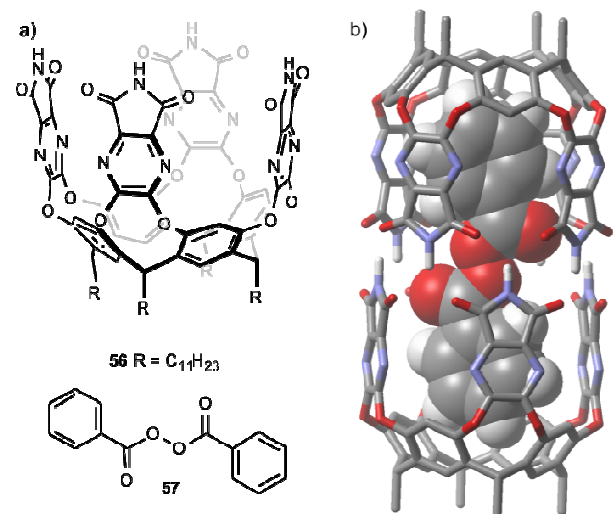


**Figure 22.** a) Line-drawing structure of cavitand **56** and benzoyl peroxide **57**. b) Energy-minimized (MM3) structure of the capsule **57**⊂**56**<sub>2</sub>. Undecyl chains at the lower rim of the cavitand components were truncated to methyl groups for simplicity.

Benzoyl peroxide is a radical initiator that is thermally unstable and decomposes within 3 hours at 70 °C through formation of two benzoyloxy radicals followed by decarboxylation. Interestingly, mesitylene-*d*<sub>12</sub> solutions of the capsule **57**⊂**56**<sub>2</sub> were stable during at least three days at 70 °C and during weeks at room temperature. In addition, whereas PPh<sub>3</sub> is quickly oxidized by benzoyl peroxide, no oxidation of the phosphine was observed when **57** was encapsulated in the dimer **56**<sub>2</sub>, even heating the solution at 70 °C and in the presence of a ten molar excess of PPh<sub>3</sub>. The addition of guests that compete with the encapsulation of **57** in the dimer or protic solvents that disrupt its intermolecular hydrogen bonding array (i.e. DMF, acetic acid) resulted in the release of benzoyl peroxide to the bulk where it underwent decomposition at its usual rate. Rebek proposed two mechanisms that could contribute to the stabilization of the radical initiator: either the confined guest could not dissociate into radicals, owing to a high energy barrier for the confined reaction, or the dissociation reaction took place but the radical recombination was faster than the decarboxylation reaction.

Rebek also described the encapsulation of the tropylium cation **47** (Figure 18a) within the cavity of a dimeric pyrogallol[4]arene capsule.<sup>85</sup> Pyrogallol[4]arene **58** (Figure 23a) formed solvent-mediated dimeric capsules that were stabilized by hydrogen bonding interactions between the hydroxyl groups at its upper rim and bridging water or methanol molecules.

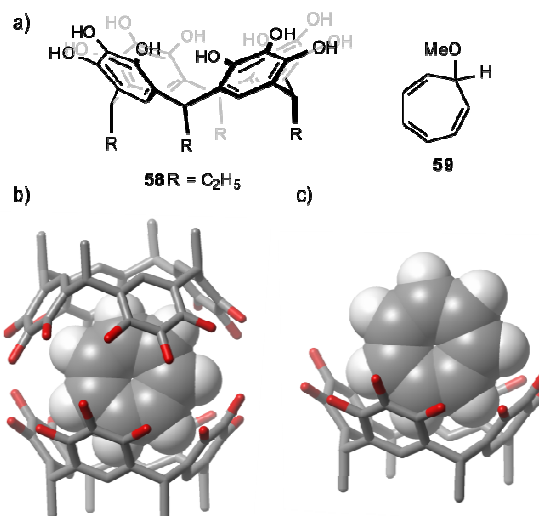


**Figure 23.** a) Line-drawing structure of pyrogallol[4]arene **58**. Energy-minimized (MM3) structures of the b) capsule **47**⊂**58**<sub>2</sub> and c) 1:1 inclusion complex **47**⊂**58**. Hydrogen atoms of the host, water and methanol molecules were removed for clarity.

A methanol solution of pyrogallol[4]arene **58** and tropylium tetrafluoroborate in 2:1 molar ratio produced a <sup>1</sup>H NMR spectrum with the expected signals for the encapsulation complex **47**⊂**58**<sub>2</sub> (Figure 23b). In the presence of methanol, the tropylium cation formed the addition product **59**. However, the methanol solutions of the **47**⊂**58**<sub>2</sub> capsule did not produce the methanolysis product. This result evidenced the stabilization of the reactive cation in the capsule's interior. The addition of pyrogallol[4]arene **58** in excess (4 equiv.) disrupted the capsule's formation and induced the assembly of a 1:1 inclusion complex with the tropylium cation (Figure 23c). In this latter complex, the cation was exposed to molecules of the bulk solution and quickly decomposed affording product **59**.

### Detection of reaction intermediates within the cavity of resorcin[4]arene derived cavitands

Rebek designed an elegant strategy to detect and stabilize elusive reaction intermediates. To this end, resorcin[4]arene cavitands with one introverted functionality were prepared. The transient species were observed and stabilized when the bound guest reacted with the introverted functionality forming a covalent host-guest complex. The stabilization of the reacting species was the result of its confinement in a reduced space

that excluded the presence of solvent or other reacting molecules. The first reported example was the stabilization of hemiaminals using a self-folding deep resorcin[4]arene cavita nd bearing an introverted aldehyde group.<sup>14</sup>

Addition of a nucleophile to an aldehyde carbonyl group produces a tetrahedral carbon intermediate that rapidly undergoes water elimination to recover the double bond involving the electrophilic carbon. An archetypal example of this type of reaction is the addition of primary amines to aldehydes affording imines through a hemiaminal intermediate (Figure 24a).

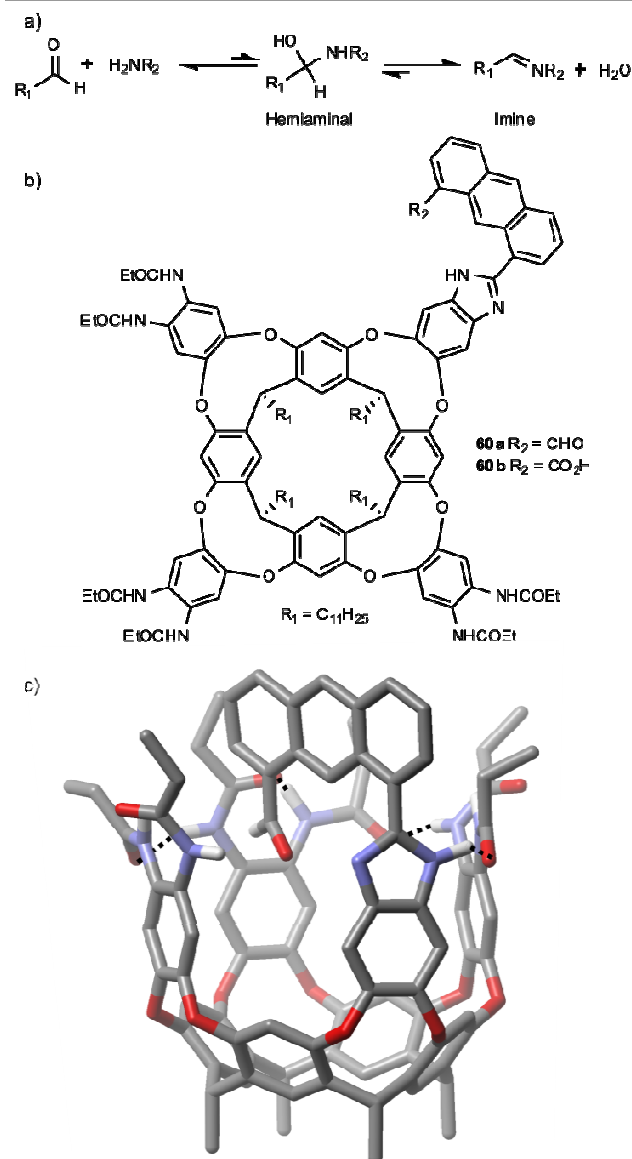
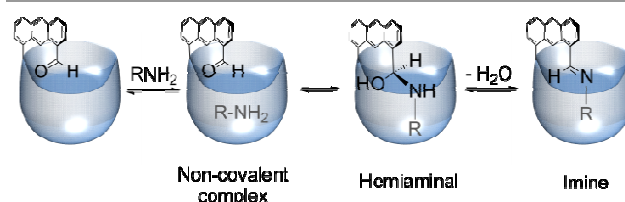


**Figure 24.** a) Equilibria involving the imine formation. b) Line-drawing structure of cavita nds **60** prepared by Rebek. c) Energy-minimized (MM3) structure of cavita nd **60a** in the vase conformation with the rotatable aldehyde arm in introverted position. Non-polar hydrogens were removed for clarity. Undecyl chains at the lower rim were truncated to methyl groups and selected hydrogen bonds in the hydrogen-bonded array of amide groups at the upper rim are marked with dashed lines.

Hemiaminals are rarely observed<sup>86</sup> in solution because the formation of a new bond does not compensate energetically the cleavage of the imine double bond. In addition, the entropic cost of bringing together the two reactants also disfavors the formation of the hemiaminal, which rapidly reverts to the starting carbonyl and amine or proceeds towards the imine with loss of water. Rebek et al. designed a self-folding resorcin[4]arene cavita nd decorated with an aldehyde-functionalized arm (**60a**). The functionalized arm experienced a fast rotation on the NMR timescale through a single C-C bond that exchanged the location of the aldehyde group between an introverted and an extroverted position towards the aromatic cavity of the cavita nd (Figure 24b).<sup>14,87</sup> The six amide groups located at the upper rim of cavita nds **60** locked the cavita nd in the vase conformation through a seam of hydrogen bonds creating a cavity ideal for the accommodation of appropriately sized guests that were isolated from the bulk solution (Figure 24c).<sup>88</sup>

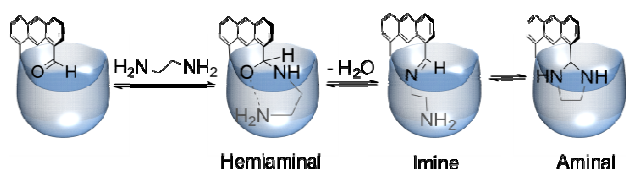
The addition of primary amines to mesitylene-*d*<sub>12</sub> millimolar solutions of cavita nd **60a** produced the folding of the cavita nd around the amine's surface (non-covalent complex, Scheme 2). Mesitylene is too bulky and cannot be accommodated within the aromatic cavity of the receptor. For this reason, cavita nd **60** resided in mesitylene solution in an open and ill-defined conformation. Upon the addition of the amine, the cavita nd adopted the vase conformation with the amine deep included in its cavity. Next, the rotatable aldehyde-functionalized arm was locked in the introverted position by reacting with the included amine and formed a hemiaminal. Eventually, the hemiaminal dehydrated within the cavity giving rise to the imine product. Remarkably, each one of the species was observable as a set of separate proton signals in the <sup>1</sup>H NMR (slow-exchange kinetics in the NMR timescale). The labile hemiaminal was observed in solution for up to 90 min, in the case of isopropylamine. Moreover, the dehydration step (imine formation) was catalyzed in the cavita nd's cavity. For isopropylamine, the imine formation was 50-fold faster when occurred within the cavity of **60a**.



**Scheme 2.** Schematic representation of the different steps that could be observed in the cavity of **60a** after the addition of a primary amine.

It is worth noting that different primary amines had diverse behaviors in the presence of container **60a**. The addition of small amines (propylamine, butylamine) to a millimolar mesitylene-*d*<sub>12</sub> solution of cavita nd **60a** produced sharp proton signals for the cavita nd, evidencing the formation of the non-covalent complex, which rapidly evolved towards the hemiaminal formation. The cavita nd **60a** is an example of a chiral concave molecule as a result of the unidirectional sense

of rotation of the hydrogen-bonded amide groups at its upper rim. Due to the asymmetric magnetic environment of the cavity, the methyne proton of the hemiaminal appeared as two separated proton signals, corresponding to the two racemic diastereomeric complexes formed in solution. The effect of the cavity's desymmetrization was more pronounced for propylamine ( $\Delta\delta = 6\text{Hz}$ ) than for butylamine ( $\Delta\delta = 1\text{Hz}$ ). This observation was explained by considering that the benzimidazole arm suffered a slight bending to better accommodate the larger guest within the cavity. Thus, in the case of the shorter propylamine, the hemiaminal was placed deeper into the cavity, bringing the methyne proton closer to the hydrogen-bonding belt of amide groups (asymmetry source). On the other hand, addition of larger amines, such as cyclohexylmethylamine, to a millimolar mesitylene- $d_{12}$  solution of cavitand **60a** did not produce immediately sharp and well-defined proton signals for the host. After some time, the signals of the  $^1\text{H}$  NMR spectrum sharpened and evidenced the formation of the imine within the cavity. Most likely, larger imines were not suitably-sized templates for the cavitand's vase conformer. The imine formation took place in the unfolded form of the cavitand. Only after the dehydration step the cavitand folded and included the covalently attached amine's scaffold. In this case and as could be expected, the intermediate hemiaminal species was not detected. A special behavior occurred on addition of ethylenediamine or ethanolamine to mesitylene- $d_{12}$  solutions of cavitand **60a**. The  $^1\text{H}$  NMR spectra showed immediately the formation of the hemiaminals (non-covalent complexes were not observed) and after 7 days only half of the hemiaminal had dehydrated to the imine. These results constitute remarkable examples of the stabilization of labile tetrahedral intermediates. The terminal non-reacted  $\text{NH}_2$  and  $\text{OH}$  groups of the amines were deeply included in the aromatic cavity of the cavitand and established intramolecular hydrogen bonds with the  $\text{OH}$  group of the hemiaminal function (Scheme 3). These highly stable hemiaminals could be detected even in the gas phase by HRMS. Imines formed completely by heating the solutions at  $70\text{ }^\circ\text{C}$  for 2 hours. Surprisingly, the predominant products after dehydration were the linear imines. Only in the case of ethylenediamine a small amount of the cyclic aminal was observed. The authors attributed the absence of cyclic aminal formation to the poor fit of the five-membered ring with the cavity size compared to the linear imines.



**Scheme 3.** Reaction scheme of the imine formation within cavitand **60a** when ethylenediamine was used.

When the same experiments were performed in toluene- $d_8$  (a competitive solvent for the receptor's cavity in the vase form) a completely different outcome was obtained. After the

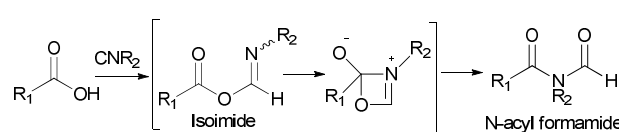
addition of hexylamine, only the proton signals corresponding to the imine were detected in the  $^1\text{H}$  NMR spectrum of the mixture. The imine formation took place outside of the cavity (the aldehyde arm adopted the extroverted position), and no hemiaminal was detected. As could be expected from this mechanism the formation of the imine was not accelerated in the presence of the cavitand.

A detailed kinetic study of the imine formation reactions shed some light on the stabilization of the hemiaminal intermediate. For the cavitand, the concentration of hemiaminal increased initially and was followed by a decline over time. Conversely, the intermolecular imine formation (reaction in the absence of cavitand) followed a steady-state kinetics approximation (the concentration of hemiaminal could be assumed as zero). In the presence of cavitand, the formation of hemiaminal from the non-covalent complex produced a rapid increase in its concentration. The subsequent dehydration step yielded the imine and caused the disappearance of the hemiaminal following a first-order kinetics. The rate of the dehydration reaction was strongly dependent on the nature of the amine. The dehydration reaction of hydrogen bonded hemiaminals such as ethylenediamine ( $t_{1/2} = 59\text{ h}$ ) or ethanolamine ( $t_{1/2} = 94$ ) was very slow due to the existence of intramolecular hydrogen bonds (enthalpic stabilization, Scheme 3) between the hemiaminal and the terminal  $\text{NH}$  and  $\text{OH}$  group. Linear hemiaminals (propylamine, butylamine, isobutylamine) showed  $t_{1/2} \approx 30\text{ min}$  for the dehydration step. On the other hand,  $\alpha$ -substituted hemiaminals (isopropylamine, cyclopropylamine, cyclobutylamine) showed dehydration rates that were 4-10 times slower than those of the unsubstituted amines. The cavitand acted as a synthetic enzyme, bringing together the two reactants (almost no entropic cost for the hemiaminal formation, practically an intramolecular reaction) and besides, the enthalpic cost of the transition state was also reduced due to the stabilization of the tetrahedral intermediates through the formation of hydrogen bonding interactions with the  $\text{NH}$  and  $\text{OH}$  groups of the hemiaminal and the belt of head-to-tail oriented amides. To explain the observed differences in reactivity of  $\alpha$ -substituted and unsubstituted amines the authors considered the structural modification experienced by the cavitand scaffold on going from the hemiaminal to the imine function. The dehydration of bulkier hemiaminals ( $\alpha$ -substituted) required a slight distortion of the walls of the cavitand, which provoked an extra-stabilization of the tetrahedral intermediate. Impressively, the detection of labile tetrahedral intermediates in natural enzymes was only possible at cryogenic temperatures<sup>89</sup> hampering the study of enzymatic mechanisms. In contrast, synthetic receptor **60a** allowed the detection of the labile hemiaminal intermediates at room temperature and at millimolar concentrations.

The results of detailed computational studies of the reaction between **60a** and isobutylamine were useful to dissect different stabilization contributions.<sup>90</sup> These studies revealed that the formation of the non-covalent complex is enthalpically driven owing to the formation of one hydrogen bond between the  $\text{NH}$  group of the amine and one  $\text{C}=\text{O}$  group

of the amides at the upper rim. The formation of the hemiaminal was favorable both from enthalpically and entropically viewpoints, but the main component was of enthalpic nature: two hydrogen bonds were formed in the transition state (between the NH and OH of the hemiaminal and the amide groups at the upper rim) and just one in the initial non-covalent complex. The hemiaminal underwent two isomerization steps prior the dehydration. Firstly, the OH group of the hemiaminal faced the wall of the cavitand, and secondly, it established a hydrogen-bonding interaction with the NH of one amide group. Finally, the dehydration reaction followed a stepwise mechanism. The NH group of an amide protonated the OH of the hemiaminal and then the deprotonated amide took back a proton from the NH group of the hemiaminal. In this way, the cavitand could be considered as an acid/base catalyst in the imine formation.

In a closely related form, Rebek et al. designed cavitand **60b**. This cavitand was elaborated with an introverted carboxylic acid function<sup>91</sup> that allowed the detection of the elusive intermediate formed in the reaction between an isonitrile group and a carboxylic acid (Scheme 4).



**Scheme 4.** Formylation of secondary amides by the reaction of a carboxylic acid and an isonitrile group. The reaction path proceeds through the elusive *O*-acyl isoimide intermediate followed by a 1,3-*O*→*N* acyl transfer (Mumm rearrangement).

The reaction between carboxylic acids and isonitriles proceeds efficiently at elevated temperatures to afford diverse *N*-acyl formamides.<sup>92</sup> In contrast, the reaction within the cavity of **60b** took place at room temperature and at millimolar concentration. Addition of isopropyl isonitrile **61** (Figure 25b) to a mesitylene-*d*<sub>12</sub> solution of cavitand **60b** produced a well-defined <sup>1</sup>H NMR spectrum indicative of the folding of the cavitand around the isonitrile. Immediately, two different sets of proton signals were visible in the spectrum that could be assigned to complexes containing the intermediate isoimide and the imide product. After a few hours, the proton signals of the isoimide complex disappeared in favor of those of the imide complex. The imide complex was detected in the gas phase by ESI-HRMS. The stabilized isoimide intermediate could be also characterized by IR spectroscopy. A carbonyl band centered at 1771 cm<sup>-1</sup> disappeared over time in favor of a new carbonyl band with maximum at 1696 cm<sup>-1</sup>. The latter C=O band was assigned to the *N*-acyl formamide. This example of labile intermediate stabilization is similar to the one previously discussed. In the reduced space provided by the cavitand's cavity both functional groups (CN and COOH) were close in space and their reaction became intramolecular from an entropic standpoint. In addition, the amide groups at the upper rim of the cavitand exerted an enthalpic stabilization of the transition state through the formation of hydrogen bonding interactions. Finally, the confined isoimide

intermediate found difficulties to rearrange due to the constriction effect of the cavitand walls.

In another turn of the screw, Rebek et al. performed the aforementioned reaction between a carboxylic acid and an isonitrile within the molecular capsule **56**<sub>2</sub> (Figure 22a).<sup>93</sup> Due to the analogy with the former example we have decided to include this stabilization process here rather than in the above hydrogen-bonded capsules section. The addition of equimolar amounts of isopropyl isonitrile **61** and *p*-tolylacetic acid **62** to a mesitylene-*d*<sub>12</sub> solution of cavitand **56** produced the quantitative self-assembly of the hetero-inclusion capsular assembly (**61-62**)<sub>2</sub>**56**<sub>2</sub> (Figure 25c). The methyl group of **62** and the isopropyl group of **61** were good fits to the resorcin[4]arene tapered ends of the capsule in terms of size and shape. Most likely, the selective formation of the hetero-inclusion assembly was due to a better occupancy of the interior of the capsule by a molecule of isonitrile **61** and a molecule of acid **62** than in the case of the corresponding homo-inclusion assemblies, **61**<sub>2</sub>**56**<sub>2</sub> and **62**<sub>2</sub>**56**<sub>2</sub>. The proximity of both functional groups near the capsular equatorial array of hydrogen bonds allowed the detection of the elusive isoimide intermediate.

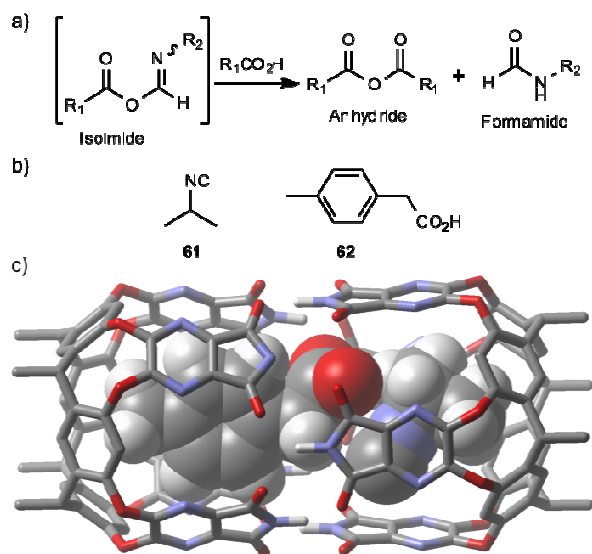


**Figure 25.** a) Scheme of the reaction between isoimides and carboxylic acids to produce an anhydride and a formamide molecule. b) Line-drawing structure of the molecules used by Rebek. c) Energy-minimized (MM3) structure of the capsular assembly (**61-62**)<sub>2</sub>**56**<sub>2</sub>. Non-polar hydrogen atoms of the host (stick representation) were removed for clarity and undecyl chains truncated to methyl groups. Bound guest shown as CPK model.

In striking contrast with the example using cavitand **60b**, the rearrangement product, the *N*-acyl formamide, was not observed. The constrictive and confined space within the cylindrical capsule precluded the rearrangement of the isoimide intermediate to yield the *N*-acyl formamide by-product. Most likely, the energy barrier of the transition state rearrangement in the capsule's cavity was very high. Because of the labile nature of the hydrogen bonds, the kinetic stability

of the complex between the stabilized isoimide and capsule **56<sub>2</sub>** was not very high. This meant that the included isoimide was in chemical exchange between the bulk solution and the capsule interior. The released isoimide intermediate reacted with excess *p*-tolylacetic acid **62** present in the bulk solution yielding the corresponding formamide and a symmetrical anhydride (Figure 25a). Simple kinetic studies proved that the formation of the isoimide intermediate within the cavity was irreversible: the capsule was a source of reactive isoimide that slowly leaked into the bulk solution to react with excess of acid. In conclusion, the outcome of the reaction of isonitriles with carboxylic acids was different in the cavity of cavitand **60b** than in the internal volume of capsule **56<sub>2</sub>**. These results highlighted the key role played by the molecular containers in the stabilization of reactive intermediates.

## Conclusions

The altered properties experienced by guests encapsulated in molecular containers have attracted the interest of many supramolecular chemists since the early reports on the topic back in the early 90's. The pioneering stabilization of cyclobutadiene reported by Cram, revealed the potential use of molecular containers as reaction vessels. Since then, he and many others have reported the stabilization of a plethora of reactive guests by encapsulation or inclusion in synthetic molecular containers. Whereas the first examples exclusively relied on the stabilization of kinetically trapped species by means of constrictive binding, more recently the stabilization of reactive species by reversible inclusion in self-assembled molecular containers (some of them even featuring polar functionalized cavities) has been put in the spotlight. In this review, we discussed remarkable examples of reactive guests' stabilization by confinement in synthetic molecular containers. The selected examples cover a period of time spanning from the beginnings of the field to the present day. Finally, we also commented the stabilization and detection of reaction intermediates through the formation of thermodynamically stable and covalent host-guest complexes with functionalized resorcin[4]arene cavitands featuring introverted polar groups. All the described examples constitute beautiful depictions of one of the most interesting applications of synthetic molecular containers.

## Acknowledgements

We thank Gobierno de España MINECO (CTQ2014-56295-R), Severo Ochoa Excellence Accreditation (2014-2018 SEV-2013-0319), FEDER funds (CTQ2014-56295-R) and the ICIQ Foundation for financial support. A.G. thanks MINECO for a FPU fellowship

## References

- 1 B. Breiner, J. K. Clegg and J. R. Nitschke, *Chem. Sci.*, 2011, **2**, 51-56.
- 2 M. Yoshizawa, J. K. Klosterman and M. Fujita, *Angew. Chem., Int. Ed.*, 2009, **48**, 3418-3438.
- 3 J. Chen and J. Rebek, *Org. Lett.*, 2002, **4**, 327-329.
- 4 D. Ma, G. Hettiarachchi, D. Nguyen, B. Zhang, J. B. Wittenberg, P. Y. Zavalij, V. Briken and L. Isaacs, *Nature Chem.*, 2012, **4**, 503-510.
- 5 T. C. Lee, E. Kalenius, A. I. Lazar, K. I. Assaf, N. Kuhnert, C. H. Grun, J. Janis, O. A. Scherman and W. M. Nau, *Nature Chem.*, 2013, **5**, 376-382.
- 6 M. Juricek, N. L. Strutt, J. C. Barnes, A. M. Butterfield, E. J. Dale, K. K. Baldridge, J. F. Stoddart and J. S. Siegel, *Nature Chem.*, 2014, **6**, 222-228.
- 7 W. M. Hart-Cooper, C. Zhao, R. M. Triano, P. Yaghoubi, H. L. Ozores, K. N. Burford, F. D. Toste, R. G. Bergman and K. N. Raymond, *Chem. Sci.*, 2015, **6**, 1383-1393.
- 8 L. Catti, Q. Zhang and K. Tiefenbacher, *Synthesis*, 2015, **48**, 0000-0000.
- 9 S. Giust, G. La Sorella, L. Sporni, F. Fabris, G. Strukul and A. Scarso, *Asian J. Org. Chem.*, 2015, **4**, 217-220.
- 10 Q. Zhang and K. Tiefenbacher, *Nat. Chem.*, 2015, **7**, 197-202.
- 11 R. M. Yebeutchou and E. Dalcanale, *J. Am. Chem. Soc.*, 2009, **131**, 2452-2453.
- 12 S. Giust, G. La Sorella, L. Sporni, G. Strukul and A. Scarso, *Chem. Commun. (Cambridge, U. K.)*, 2015, **51**, 1658-1661.
- 13 Q. Zhang and K. Tiefenbacher, *J. Am. Chem. Soc.*, 2013, **135**, 16213-16219.
- 14 T. Iwasawa, R. J. Hooley and J. Rebek, *Science*, 2007, **317**, 493-496.
- 15 D. Fiedler, R. G. Bergman and K. N. Raymond, *Angew. Chem., Int. Ed.*, 2006, **45**, 745-748.
- 16 Q. K. Liu, J. P. Ma and Y. B. Dong, *J. Am. Chem. Soc.*, 2010, **132**, 7005-7017.
- 17 G. H. Ning, Y. Inokuma and M. Fujita, *Chem.--Asian J.*, 2014, **9**, 466-468.
- 18 C. Schwarzmaier, A. Schindler, C. Heindl, S. Scheuermayer, E. V. Peresyphkina, A. V. Virovets, M. Neumeier, R. Gschwind and M. Scheer, *Angew. Chem., Int. Ed.*, 2013, **52**, 10896-10899.
- 19 T. Kawamichi, T. Haneda, M. Kawano and M. Fujita, *Nature*, 2009, **461**, 633-635.
- 20 Y. Y. Li, F. Gao, J. E. Beves, Y. Z. Li and J. L. Zuo, *Chem. Commun. (Cambridge, U. K.)*, 2013, **49**, 3658-3660.
- 21 L. S. Kaanumalle, J. Nithyanandhan, M. Pattabiraman, N. Jayaraman and V. Ramamurthy, *J. Am. Chem. Soc.*, 2004, **126**, 8999-9006.
- 22 R. Eelkema, K. Maeda, B. Odell and H. L. Anderson, *J. Am. Chem. Soc.*, 2007, **129**, 12384-12385.
- 23 Y. Liu, J. Shi, Y. Chen and C. F. Ke, *Angew. Chem., Int. Ed.*, 2008, **47**, 7293-7296.
- 24 I. Manet, S. Monti, P. Bortolus, M. Fagnoni and A. Albini, *Chem.--Eur. J.*, 2005, **11**, 4274-4282.
- 25 J. Shi, Y. Chen, Q. A. Wang and Y. Liu, *Adv. Mater. (Weinheim, Ger.)*, 2010, **22**, 2575-2578.
- 26 W. Wei, W. L. Li, Z. F. Li, W. P. Su and M. C. Hong, *Chem.--Eur. J.*, 2013, **19**, 468-472.
- 27 L. Trembleau and J. Rebek, *Science*, 2003, **301**, 1219-1220.
- 28 D. Fiedler, R. G. Bergman and K. N. Raymond, *Angew. Chem., Int. Ed.*, 2004, **43**, 6748-6751.
- 29 S. Tashiro, M. Kobayashi and M. Fujita, *J. Am. Chem. Soc.*, 2006, **128**, 9280-9281.
- 30 S. Tashiro, M. Tominaga, Y. Yamaguchi, K. Kato and M. Fujita, *Angew. Chem., Int. Ed.*, 2006, **45**, 241-244.
- 31 H. Takezawa, T. Murase and M. Fujita, *J. Am. Chem. Soc.*, 2012, **134**, 17420-17423.

- 32 T. Kusukawa and M. Fujita, *J. Am. Chem. Soc.*, 1999, **121**, 1397-1398.
- 33 D. A. Makeiff, K. Vishnumurthy and J. C. Sherman, *J. Am. Chem. Soc.*, 2003, **125**, 9558-9559.
- 34 T. Iwasawa, E. Mann and J. Rebek, *J. Am. Chem. Soc.*, 2006, **128**, 9308-9309.
- 35 A. Scarso and J. Rebek, *J. Am. Chem. Soc.*, 2004, **126**, 8956-8960.
- 36 J. M. Shen, M. C. Kung, Z. L. Shen, Z. Wang, W. A. Gunderson, B. M. Hoffman and H. H. Kung, *J. Am. Chem. Soc.*, 2014, **136**, 5185-5188.
- 37 K. Ono, M. Yoshizawa, M. Akita, T. Kato, Y. Tsunobuchi, S. Ohkoshi and M. Fujita, *J. Am. Chem. Soc.*, 2009, **131**, 2782-2783.
- 38 K. Nakabayashi, M. Kawano, M. Yoshizawa, S. Ohkoshi and M. Fujita, *J. Am. Chem. Soc.*, 2004, **126**, 16694-16695.
- 39 M. Yoshizawa, T. Kusukawa, M. Kawano, T. Ohhara, I. Tanaka, K. Kurihara, N. Niimura and M. Fujita, *J. Am. Chem. Soc.*, 2005, **127**, 2798-2799.
- 40 T. Sawada, M. Yoshizawa, S. Sato and M. Fujita, *Nature Chem.*, 2009, **1**, 53-56.
- 41 I. A. Riddell, M. M. J. Smulders, J. K. Clegg and J. R. Nitschke, *Chem. Commun. (Cambridge, U. K.)*, 2011, **47**, 457-459.
- 42 M. L. Merlau, M. D. P. Mejia, S. T. Nguyen and J. T. Hupp, *Angew. Chem., Int. Ed.*, 2001, **40**, 4239-4242.
- 43 W. M. Hart-Cooper, K. N. Clary, F. D. Toste, R. G. Bergman and K. N. Raymond, *J. Am. Chem. Soc.*, 2012, **134**, 17873-17876.
- 44 M. D. Pluth, R. G. Bergman and K. N. Raymond, *J. Am. Chem. Soc.*, 2007, **129**, 11459-11467.
- 45 W. Y. Sun, T. Kusukawa and M. Fujita, *J. Am. Chem. Soc.*, 2002, **124**, 11570-11571.
- 46 T. H. Wong, J. C. Chang, C. C. Lai, Y. H. Liu, S. M. Peng and S. H. Chiu, *J. Org. Chem.*, 2014, **79**, 3581-3586.
- 47 D. J. Cram, S. Karbach, Y. H. Kim, L. Baczynskyj and G. W. Kallemeyn, *J. Am. Chem. Soc.*, 1985, **107**, 2575-2576.
- 48 M. L. C. Quan and D. J. Cram, *J. Am. Chem. Soc.*, 1991, **113**, 2754-2755.
- 49 R. G. Chapman, N. Chopra, E. D. Cochien and J. C. Sherman, *J. Am. Chem. Soc.*, 1994, **116**, 369-370.
- 50 J. C. Sherman and D. J. Cram, *J. Am. Chem. Soc.*, 1989, **111**, 4527-4528.
- 51 D. J. Cram, M. E. Tanner and R. Thomas, *Angew. Chem., Int. Ed. Engl.*, 1991, **30**, 1024-1027.
- 52 O. L. Chapman, C. L. McIntosh and J. Pacansky, *J. Am. Chem. Soc.*, 1973, **95**, 614-617.
- 53 R. Warmuth, *Chem. Commun. (Cambridge, U. K.)*, 1998, 59-60.
- 54 H. H. Wenk, M. Winkler and W. Sander, *Angew. Chem., Int. Ed.*, 2003, **42**, 502-528.
- 55 H. J. Jiao, P. V. Schleyer, B. R. Beno, K. N. Houk and R. Warmuth, *Angew. Chem., Int. Ed.*, 1997, **36**, 2761-2764.
- 56 R. Warmuth and M. A. Marvel, *Angew. Chem., Int. Ed.*, 2000, **39**, 1117-1119.
- 57 R. Warmuth and M. A. Marvel, *Chem.--Eur. J.*, 2001, **7**, 1209-1220.
- 58 X. J. Liu, G. S. Chu, R. A. Moss, R. R. Sauers and R. Warmuth, *Angew. Chem., Int. Ed.*, 2005, **44**, 1994-1997.
- 59 R. Warmuth and S. Makowiec, *J. Am. Chem. Soc.*, 2005, **127**, 1084-1085.
- 60 R. Warmuth and S. Makowiec, *J. Am. Chem. Soc.*, 2007, **129**, 1233-1241.
- 61 P. Roach and R. Warmuth, *Angew. Chem., Int. Ed.*, 2003, **42**, 3039-3042.
- 62 N. Nishimura and K. Kobayashi, *J. Org. Chem.*, 2010, **75**, 6079-6085.
- 63 Y. C. Horng, P. S. Huang, C. C. Hsieh, C. H. Kuo and T. S. Kuo, *Chem. Commun. (Cambridge, U. K.)*, 2012, **48**, 8844-8846.
- 64 C. Y. Gao, L. Zhao and M. X. Wang, *J. Am. Chem. Soc.*, 2012, **134**, 824-827.
- 65 A. Galan, G. Gil-Ramirez and P. Ballester, *Org. Lett.*, 2013, **15**, 4976-4979.
- 66 J. C. Craig, N. N. Ekwuribe and L. D. Gruenke, *Tetrahedron Lett.*, 1979, 4025-4028.
- 67 A. H. Khuthier, M. A. Aliraqi, G. Hallstrom and B. Lindeke, *J. Chem. Soc., Chem. Commun.*, 1979, 9-10.
- 68 M. Fujita, D. Oguro, M. Miyazawa, H. Oka, K. Yamaguchi and K. Ogura, *Nature*, 1995, **378**, 469-471.
- 69 M. Yoshizawa, T. Kusukawa, M. Fujita and K. Yamaguchi, *J. Am. Chem. Soc.*, 2000, **122**, 6311-6312.
- 70 M. Yoshizawa, T. Kusukawa, M. Fujita, S. Sakamoto and K. Yamaguchi, *J. Am. Chem. Soc.*, 2001, **123**, 10454-10459.
- 71 S. Y. Yu, T. Kusukawa, K. Biradha and M. Fujita, *J. Am. Chem. Soc.*, 2000, **122**, 2665-2666.
- 72 A related cavity-controlled polymerization was described in T. Murase, S. Sato and M. Fujita, *Angew. Chem., Int. Ed.*, 2007, **46**, 1083-1085.
- 73 M. Kawano, Y. Kobayashi, T. Ozeki and M. Fujita, *J. Am. Chem. Soc.*, 2006, **128**, 6558-6559.
- 74 R. Poli, *Chem. Rev. (Washington, DC, U. S.)*, 1996, **96**, 2135-2204.
- 75 S. Horiuchi, T. Murase and M. Fujita, *J. Am. Chem. Soc.*, 2011, **133**, 12445-12447.
- 76 M. Ziegler, J. L. Brumaghim and K. N. Raymond, *Angew. Chem., Int. Ed.*, 2000, **39**, 4119-4121.
- 77 D. L. Caulder, R. E. Powers, T. N. Parac and K. N. Raymond, *Angew. Chem., Int. Ed.*, 1998, **37**, 1840-1843.
- 78 J. L. Brumaghim, M. Michels and K. N. Raymond, *Eur. J. Org. Chem.*, 2004, 4552-4559.
- 79 V. M. Dong, D. Fiedler, B. Carl, R. G. Bergman and K. N. Raymond, *J. Am. Chem. Soc.*, 2006, **128**, 14464-14465.
- 80 J. L. Brumaghim, M. Michels, D. Pagliero and K. N. Raymond, *Eur. J. Org. Chem.*, 2004, 5115-5118.
- 81 P. Mal, B. Breiner, K. Rissanen and J. R. Nitschke, *Science*, 2009, **324**, 1697-1699.
- 82 M. Yamashina, Y. Sei, M. Akita and M. Yoshizawa, *Nat. Commun.*, 2014, **5**.
- 83 T. Heinz, D. M. Rudkevich and J. Rebek, *Nature*, 1998, **394**, 764-766.
- 84 S. K. Korner, F. C. Tucci, D. M. Rudkevich, T. Heinz and J. Rebek, *Chem.--Eur. J.*, 2000, **6**, 187-195.
- 85 A. Shivanyuk, J. C. Frieese, S. Doring and J. Rebek, *J. Org. Chem.*, 2003, **68**, 6489-6496.
- 86 D. A. Evans, G. Borg and K. A. Scheidt, *Angew. Chem., Int. Ed.*, 2002, **41**, 3188-3191.
- 87 R. J. Hooley, T. Iwasawa and J. Rebek, *J. Am. Chem. Soc.*, 2007, **129**, 15330-15339.
- 88 For an example of the acceleration of a  $S_NAr$  reaction by the stabilization of the reaction intermediate (Meisenheimer complex) by the amide groups at the upper rim of a resorcin[4]arene cavitand view S. M. Butterfield and J. Rebek, *Chem. Commun. (Cambridge, U. K.)*, 2007, 1605-1607.
- 89 A. Heine, G. DeSantis, J. G. Luz, M. Mitchell, C. H. Wong and I. A. Wilson, *Science*, 2001, **294**, 369-374.

90 L. Xu, S. G. Hua and S. H. Li, *Chem. Commun. (Cambridge, U. K.)*, 2013, **49**, 1542-1544.

91 P. Restorp and J. Rebek, *J. Am. Chem. Soc.*, 2008, **130**, 11850-11851.

92 X. C. Li and S. J. Danishefsky, *J. Am. Chem. Soc.*, 2008, **130**, 5446-5448.

93 J. L. Hou, D. Ajami and J. Rebek, *J. Am. Chem. Soc.*, 2008, **130**, 7810-7811.